Two-quasiparticle and single-phonon states of even–even deformed nuclei in the region of the actinides

S. P. Ivanova, A. L. Komov, L. A. Malov, and V. G. Solov'ev

Joint Institute for Nuclear Research, Dubna
Fiz. Elem. Chastits At. Yadra 7, 450–498 (April–June 1976)

Low-lying two-quasiparticle and single-phonon states of even–even nuclei are described in a wide range of the actinides ($228 \leq A \leq 260$) on the basis of the semimicroscopic approach. A study is made of role of anharmonic effects and it is shown that in a number of cases the two-phonon components make a large contribution to the structure of the first and second vibrational states. The experimental data are analyzed and compared with the results of theoretical calculations.

PACS numbers: 21.60.Gx, 27.90.+b, 21.10.Ma

INTRODUCTION

The present stage in the development of nuclear physics consists of the accumulation of experimental data, their analysis, and comparison with the results of calculations made by different semimicroscopic methods. The determination of the quantum numbers of the ground state and ever higher excited states of nuclei continues to occupy a central position in nuclear physics. There have now been accumulated many experimental data associated with the study of the low-lying states of a large number of nuclei, α, β, and γ transitions, and the cross sections of direct nuclear reactions. The experimental data in the region of deformed nuclei are especially extensive. The existing experimental material has been collected in Refs. 1–3 and for a number of nuclei, for example, for $A=182$ (Ref. 4) and others in the region $150 \leqslant A \leqslant 190$ (Ref. 5) it has been painstakingly analyzed.

The recently developed semimicroscopic methods of theoretical nuclear physics provide the basis for calculating the quantum numbers of the low-lying states of nuclei (see, for example, Refs. 6–8). The calculated energies and the structure of low-lying nonrotational states of even–even nuclei in the region $150 \leqslant A \leqslant 190$ and comparison of them with experimental data are given in Refs. 5 and 9 and in other publications.

Two-quasiparticle and single-phonon states of even–even deformed nuclei in the region of the actinides were calculated in Ref. 10 with the single-particle energies and wave functions of the Nilsson potential and in Ref. 11 with the Woods–Saxon single-particle potential. A fairly good description of the nonrotational states of odd deformed nuclei was obtained. However, only a small fraction of the results of calculations of the states of nuclei in the actinide region has been published.[12,13]

The present paper is devoted to the important task of giving the theoretical energies and wave functions of the nonrotational states of even–even nuclei in the actinide region and comparing them with experimental data.

1. TREATMENT OF TWO-QUASIPARTICLE AND SINGLE-PHONON STATES

We give here the main equations used to describe the two-quasiparticle and single-phonon states in even–even deformed nuclei. The model nuclear Hamiltonian is written in the form

$$H=H_{\text{av}}+H_{\text{pair}}+\sum_{\lambda,\,\mu\geqslant 0}\varkappa^{(\lambda)}Q^{+}_{\lambda\mu}Q_{\lambda\mu}/2, \tag{1}$$

where H_{av} is the average field of the proton and neutron systems described by the Woods–Saxon potential; H_{pair} is the interaction leading to pairing correlations of superconducting type; the last term in (1) describes the multipole–multipole interaction.

To describe two-quasiparticle states, one uses only part of the Hamiltonian (1), namely

$$H_0=H_{\text{av}}+H_{\text{pair}}=H_0(n)+H_0(p), \tag{2}$$

where for the neutron system

$$H_0(n)=\sum_{s\sigma}\{E(s)-\lambda_n\}a^{+}_{s\sigma}a_{s\sigma}-G_N\sum_{ss'}a^{+}_{s+}a^{+}_{s-}a_{s'-}a_{s'+}. \tag{3}$$

Here, $E(s)$ are the single-particle energies; $a_{s\sigma}$ is the operator of annihilation of a nucleon; G_N is the constant of the pairing interaction; λ_n is the chemical potential of the neutron system. In the proton system, we denote the constant of the pairing interaction and the chemical potential by G_z and λ_p. We denote the quantum numbers characterizing the single-particle state of the neutron system by $(s\sigma)$ and of the neutron and proton system by $(q\sigma)$, where $\sigma=\pm 1$.

We perform a Bogolyubov canonical transformation:

$$a_{s\sigma}=u_s\alpha_{s-\sigma}+\sigma v_s\alpha^{+}_{s\sigma}, \tag{4}$$

where $\alpha_{s\sigma}$ is the operator of absorption of a quasiparticle;

$$u_s^2+v_s^2=1. \tag{5}$$

We determine the wave function of the ground state of the system by the condition

$$\alpha_{s\sigma}\Psi_0=0. \tag{6}$$

We find the expectation value of $H_0(n)$ with respect to the state Ψ_0 using a variational principle and as a result (see Ref. 8) we obtain the following system of equations for the correlation function C_n and the chemical potential λ_n:

$$1=\frac{G_N}{2}\sum_{s}\frac{1}{\sqrt{C_n^2+(E(s)-\lambda_n)^2}}; \tag{7}$$

$$N=\sum_{s}\left\{1-\frac{E(s)-\lambda_n}{\sqrt{C_n^2+(E(s)-\lambda_n)^2}}\right\}, \tag{8}$$

where N is the number of neutrons.

The energy and wave function of the ground state of the system have the form

$$\mathscr{E}_0 = \sum_s 2E(s)\,v_s^2 - C_n^2/G_N; \tag{9}$$

$$\Psi_0 = \prod_s (u_s + v_s a_{s+}^+ a_{s-}^+)\,\Psi_{00}, \tag{10}$$

where

$$a_{s\sigma}\Psi_{00} = 0; \quad \varepsilon(s) = \sqrt{C_n^2 + [E(s) - \lambda_n]^2}; \tag{11}$$

$$u_s^2 = \{1 + [E(s) - \lambda_n]/\varepsilon(s)\}/2; \quad v_s^2 = \{1 - [E(s) - \lambda_n]/\varepsilon(s)\}/2. \tag{12}$$

In the model of independent quasiparticles, the excited states of even–even nuclei are two-quasiparticle states. At higher energies, the excitations are four-quasiparticle states, etc.

The wave function of a two-quasiparticle state with $K^\pi \neq 0^+$ has the form

$$\Psi_K^\pi(s_1, s_2) = a_{s_1\sigma_1}^+ a_{s_2\sigma_2}^+ \prod_{s \neq s_1, s_2} \{u_s(s_1, s_2) + v_s(s_1, s_2)\,a_{s+}^+ a_{s-}^+\}\,\Psi_{00}. \tag{13}$$

The correlation function $C_n(s_1, s_2)$ and the chemical potential are determined from the equations

$$1 = \frac{G_N}{2} \sum_{\substack{s \\ (s \neq s_1, s_2)}} \frac{1}{\sqrt{C_n^2(s_1, s_2) + \{E(s) - \lambda_n(s_1, s_2)\}^2}}; \tag{14}$$

$$N = 2 + \sum_{\substack{s \\ (s \neq s_1, s_2)}} \left\{1 - \frac{E(s) - \lambda_n(s_1, s_2)}{\sqrt{C_n^2(s_1, s_2) + \{E(s) - \lambda_n(s_1, s_2)\}^2}}\right\}. \tag{15}$$

The values of $C_n(s_1, s_2), \lambda_n(s_1, s_2), u_s(s_1, s_2), v_s(s_1, s_2)$ depend on the levels s_1 and s_2 at which the quasiparticles are. The energies of the two-quasiparticle states are determined by the difference

$$\mathscr{E}_0(s_1, s_2) - \mathscr{E}_0, \tag{16}$$

where

$$\mathscr{E}_0(s_1, s_2) = E(s_1) + E(s_2) + 2 \sum_{s \neq s_1, s_2} E(s)\,v_s^2(s_1, s_2) - C_n^2(s_1, s_2)/G_N. \tag{17}$$

To describe the vibrational states, one introduces the phonon operators

$$Q_g = \frac{1}{2} \sum_{q, q'} \{\psi_{qq'}^g A(q, q') - \varphi_{qq'}^g A^+(q, q')\}, \tag{18}$$

where $g = \lambda\mu j$; $A(q, q') = \sum_\sigma \sigma\alpha_{q'\sigma}\alpha_{q-\sigma}/\sqrt{2}$ (or $= \sum_\sigma \alpha_{q\sigma}\alpha_{q'\sigma}/\sqrt{2}$). The corresponding part of the Hamiltonian (1) can be written as

$$H_v = \sum_q \varepsilon(q)\,B(q, q) - \frac{1}{2} \sum_{\lambda, \mu \geqslant 0} \varkappa^{(\lambda)} \sum_{qq'} \sum_{q_2q_2'} \sum_{jj'} f^{\lambda\mu}(qq')\,f^{\lambda\mu}(q_2q_2') \times u_{qq'}u_{q_2q_2'}(\psi_{qq'}^g \mp \varphi_{qq'}^g)(\psi_{q_2q_2'}^{g'} \pm \varphi_{q_2q_2'}^{g'})\,Q_g^+ Q_{g'}. \tag{19}$$

Here $g = \lambda\mu j$; $g' = \lambda\mu j'$; $f^{\lambda\mu}(q, q')$ is the matrix element of the operator of the multipole moment $\lambda\mu$; $u_{qq'} = u_q v_{q'} + v_q u_{q'}$; $v_{qq'} = u_q u_{q'} - v_q v_{q'}$; $B(q, q') = \sum_\sigma \alpha_{q\sigma}^+ \alpha_{q'\sigma}^+$ (or $= \sum_\sigma \sigma\alpha_{q-\sigma}^+\alpha_{q'\sigma}$).

The wave function of the ground state of an even–even nucleus is defined as the no-phonon wave function, i.e., $Q_g\Psi_0 = 0$. The excited states are treated as single-phonon states and are described by the wave functions $Q_g^+\Psi_0$.

The energies ω_g and the wave functions of the single-phonon states can be found by means of a variational principle (see Ref. 8). For all single-phonon states (except 0^+ states) the secular equation has the form

$$1 = 2\varkappa^{(\lambda)} \sum_{qq'} \frac{[f^{\lambda\mu}(q, q')\,u_{qq'}]^2\,[\varepsilon(q) + \varepsilon(q')]}{[\varepsilon(q) + \varepsilon(q')]^2 - (\omega_g)^2}. \tag{20}$$

Using the condition of normalization of the wave functions, we can readily find

$$\psi_{qq'}^g = \frac{1}{\sqrt{2Y_g}} \frac{f^{\lambda\mu}(q, q')\,u_{qq'}}{\varepsilon(q) + \varepsilon(q') - \omega_g}; \tag{21}$$

$$\varphi_{qq'}^g = \frac{1}{\sqrt{2Y_g}} \frac{f^{\lambda\mu}(q, q')\,u_{qq'}}{\varepsilon(q) + \varepsilon(q') + \omega_g}; \tag{22}$$

$$Y_g = \sum_{qq'} \frac{[f^{\lambda\mu}(q, q')\,u_{qq'}]^2\,\omega_g\,[\varepsilon(q) + \varepsilon(q')]}{\{[\varepsilon(q) + \varepsilon(q')]^2 - (\omega_g)^2\}^2}. \tag{23}$$

The secular equation and the wave function of the single-phonon 0^+ state are given in Ref. 8.

2. ANHARMONICITY OF THE VIBRATIONAL STATES

Anharmonic effects in even–even deformed nuclei were studied in Refs. 8 and 14–17 with a wave function that includes two-phonon terms as well as the single-phonon term. It is shown that in strongly deformed nuclei the first vibrational states are essentially single-phonon and therefore the results of calculations in the harmonic approximation give the correct structure of these states. For $K^\pi = 0^+$ states and for the second and higher states with given K^π the anharmonic effects are more important. They increase as the nuclei approach the transition regions.

We give the main equations for describing the vibrational states with allowance for anharmonicity. The Hamiltonian (1) with allowance for the fulfilment of the secular equation (20) and the corresponding equation for the $\lambda = 2$, $\mu = 0$ states has the form

$$H = H_v + H_{vq} = \sum_g \omega_g Q_g^+ Q_g - \frac{1}{2} \sum_{q, q'} [\Gamma^g(q, q')\,B(q, q')\,(Q_g^+ + Q_g) + \text{h.c.}] + \frac{G}{4} \sum_{q, q'} v_{qq}u_{q'q'}\,[A^+(q, q)\,B(q', q') + \text{h.c.}], \tag{24}$$

where

$$\Gamma^g(q, q') = \frac{f^{\lambda\mu}(q, q')}{2\sqrt{Y_g}}\,v_{qq'}. \tag{25}$$

We write the wave function of the vibrational state in the form

$$\Psi_i(K^\pi) = \left\{\sum_g \theta_g^i Q_g^+ + \frac{1}{\sqrt{2}} \sum_{g_1g_2} \Delta_{g_1g_2}^i Q_{g_1}^+ Q_{g_2}^+\right\}\Psi_0, \tag{26}$$

where i is the number of the excited state with the given K^π. The normalization condition is

$$\sum_g (\theta_g^i)^2 + \sum_{g_1g_2} (\Delta_{g_1g_2}^i)^2 = 1. \tag{27}$$

We find the expectation value of $H_v + H_{vq}$ with respect to the state (26) and from the variational principle we obtain a secular equation in the form of a determinant in the (jj') space:

TABLE 1. Lowest vibrational states of ^{228}Th.

K_i^π	Energy, MeV Experiment	Energy, MeV Calculation	Structure, %
2_1^+	0.977	1.0	(221) 95 (301, 321) 2
2_2^+	1.154	1.6	(311, 311) 98,
0_1^-	0.328	0.4	(301) 97, (201, 301) 1
0_2^-	—	1.7	(201, 301) 99
1_1^-	0.740	0.7	(311) 97 (201, 311) 2
1_2^-		1.8	(312) 90 (201, 311) 9
2_1^-	1.123	1.2	(321) 90 (221, 301) 10
2_2^-	—	1.6	(221, 301) 90 (321) 10
0_1^+	0.830	0.9	(301, 301) 83 (201) 13 (202) 3
0_2^+	0.888	1.2	(201) 75 (301, 301) 15 (311, 311) 5 (201, 203) 3 (221, 221) 2

TABLE 2. Energy and structure of 0_1^+ and 0_2^+ states.

Nucleus	Energy, MeV Experiment	Energy, MeV Calculation	Structure, %
^{228}Th	0.830	0.9	(301, 301) 83 (201) 13 (202) 3
	0.888	1.2	(201) 75 (301, 301) 15 (311, 311) 5 (201, 203) 3 (221, 221) 2
^{230}Th	0.634	0.6	(201) 76 (201, 201) 21
	1.590	1.5	(301, 301) 91 (203) 6
^{232}Th	0.731	0.7	(201) 75 (201, 201) 19 (221, 221) 2 (301, 301) 2
		1.5	(202) 50 (301, 301) 44 (221, 221) 2 (303) 2 (201, 201) 1
^{232}U	0.691	1.1	(201) 84 (202) 2 (201, 201) 8 (301, 301) 3 (221, 221) 2
		1.5	(301, 301) 80 (203) 9 (202) 7 (201) 4
^{234}U	0.811	0.9	(201) 86 (201, 202) 8 (201, 203) 3 (201, 201) 1 (221, 221) 1
	1.046	1.2	(202) 84 (301, 301) 9 (221, 221) 2 (203) 1
^{236}U	0.920	1.0	(201) 85 (321, 321) 6 (311, 311) 4 (221, 221) 1
		1.3	(202) 74 (301, 301) 14 (311, 311) 5 (203) 3 (321, 321) 2 (201) 1
^{238}U	0.925	0.8	(201) 84 (201, 201) 12
	0.993	1.4	(202) 88 (203) 5 (301, 301) 4 (201, 202) 3
^{238}Pu	0.945	1.1	(201) 94 (301, 301) 2 (221, 221) 1
	1.134	1.2	(301, 301) 62 (202) 35 (201) 3
^{240}Pu	0.860	0.9	(201) 85 (221, 221) 5 (301, 301) 4 (201, 201) 3 (321, 321) 2
	1.411	1.2	(301, 301) 84 (203) 12 (201) 3

$$\det \| (\omega_g - \eta_i)\, \delta_{gg'} - K^i (g, g') \| = 0, \tag{28}$$

where $g = \lambda\mu j$; $g' = \lambda\mu j'$;

$$K^i (g, g') = \frac{1}{2} \sum_{g_1, g_2} \frac{U_g^{g_1 g_2} U_{g'}^{g_1 g_2}}{\omega_{g_1} + \omega_{g_2} - \eta_i}; \tag{29}$$

$$U_g^{g_1 g_2} = \langle Q_g H_{vq} Q_{g_1}^+ Q_{g_2}^+ \rangle. \tag{30}$$

From the solution of Eq. (28), we find the state energies η_i; the values of $(\theta_g^i)^2$ determine the contribution of the single-phonon components and $(\Delta^i_{g_1 g_2})^2$ the values of the two-phonon components.

The results of the calculations are given in Tables 1 and 2, which include the experimental and calculated energies and the structure of the first and second vibrational states.[16,17] The phonons are denoted by $(\lambda\mu j)$; for example, (201, 301) denotes the two-phonon component from the first roots of phonons with $\lambda\mu = 20$ and $\lambda'\mu' = 30$. As an example, we consider the nucleus ^{228}Th, for which in Table I we give the states with K_i^π equal to $0^+_{1,2}, 2^+_{1,2}, 0^-_{1,2}, 1^-_{1,2}$, and $2^-_{1,2}$. This nucleus is near the transition region, and one could expect anharmonicity to have the greatest effect in this case. It can, however, be seen that all the first vibrational states with the given K^π (except the 0^+ states) are single-phonon states, but the structure of the second vibrational states is such that the two-phonon component dominates. The large role of the two-phonon components in this nucleus is due to the very low energy of the (301) phonon and the comparatively low energy of the (311) phonon.

At the same time, the first 2^+ state of, for example, the nucleus ^{240}Pu is characterized by a large contribution of the two-phonon components (~17%).

Let us consider separately the structure of the 0^+ states. The interest in states with $K^\pi = 0^+$ is very great, and they have been studied in different approaches.[18,19] In this paper, we analyze the structure of the 0^+ states with allowance for the effect of anharmonicity.

The results of the calculations of Ref. 16 are given in Table 2. The structure of the first 0^+ states for different nuclei may be very different. For example, in the case of ^{230,232}Th, ^{234,236}U, ^{238,240}Pu the main contribution to the wave function is made by the single-phonon component (201), whereas ^{228}Th is characterized by 0_1^+ being a two-phonon state. But the influence of the two-phonon components on the lowest 0^+ state is large and in the first case their contribution fluctuates between 5 and 20%.

The second 0^+ states have a more complicated structure and they evidently depend on the choice of the interaction constants (see Table 2).

3. RESULTS OF CALCULATIONS

We give the schemes of the single-particle levels of the Woods–Saxon potential and the parameters, which were fixed during the calculations in the actinide region, and we discuss the presentation of the results of the calculations.

The calculations of the energies and wave functions of the two-quasiparticle and single-phonon states are based on the single-particle energies and wave functions of the Woods–Saxon potential. The eigenvalues of the energies and the eigenfunctions for the axisymmetric Woods–Saxon potential were calculated by the approximate method proposed in Ref. 20. The single-particle energies and wave functions are partly given in Ref. 13. Since the energies and wave functions of the single-particle levels, which are solutions of the Schrödinger equation with the Woods–Saxon potential, depend on the mass number A, the deformed nuclei are divided into zones. The nuclei we consider are divided into four zones, i.e., the energies and wave functions are calculated for $A = 229$, 239, 247, and 255. Within each zone, there are no changes in the energies and wave functions.

In order to obtain the correct order of the single-particle levels in the proton and neutron systems,

TABLE 3. Parameters of Woods–Saxon potential for nuclei in the actinide region.

A zone	Neutron systems V_0, MeV	r_0, F	α, F^{-1}	$\varkappa$, F^{-2}	Proton systems V_0, MeV	r_0, F	α, F^{-1}	$\varkappa$, F^{-2}
229	47.0	1.26	1.40	0.470	60.5	1.24	1.55	0.375
239	46.7	1.26	1.45	0.430	61.0	1.24	1.55	0.375
247	46.0	1.26	1.38	0.430	62.0	1.24	1.55	0.370
255	46.0	1.26	1.30	0.470	62.5	1.24	1.55	0.360

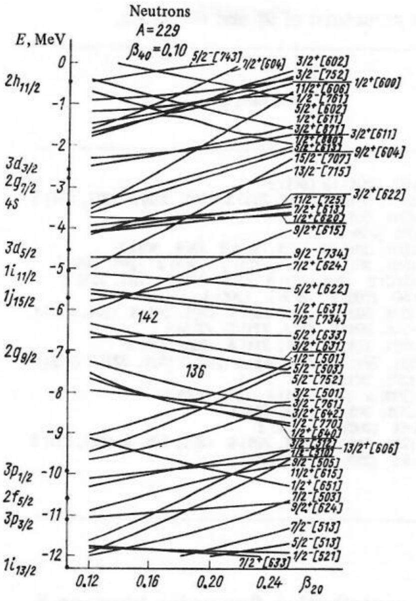

FIG. 1.

some parameters of the potential were changed somewhat from zone to zone. The parameters of the axisymmetric Woods–Saxon potential are given in Table 3. It should be noted that the parameters given in Table 3 do not differ strongly from the parameters of the Woods–Saxon potential for nuclei in the region $150 \leqslant A \leqslant 190$, which are given in Ref. 21.

The shape of the nucleus is described by

$$R(\theta) = R_0(1+\beta_0+\beta_{20}Y_{20}(\theta)+\beta_{40}Y_{40}(\theta)), \tag{31}$$

where $R_0 = r_0 A^{1/3}$ is the radius of an equally large spherical nucleus; β_0 is the constant introduced to satisfy the condition that the volume of the nucleus remain the same; β_{20} is the quadrupole deformation parameter; β_{40} is the hexadecapole deformation parameter.

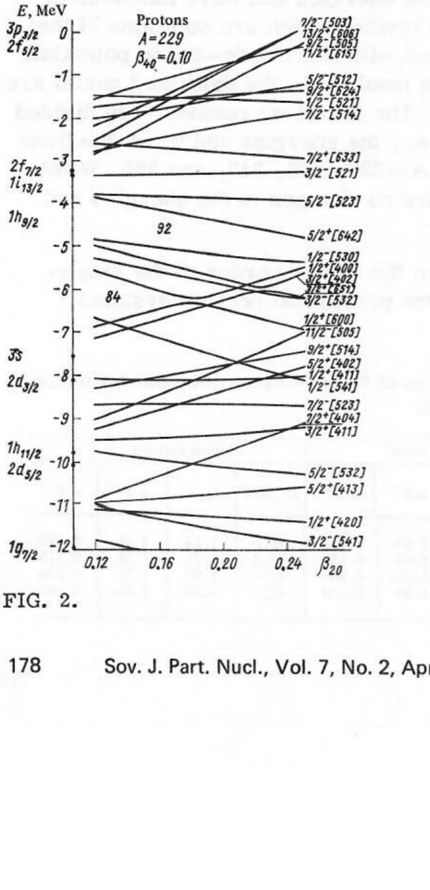

FIG. 2.

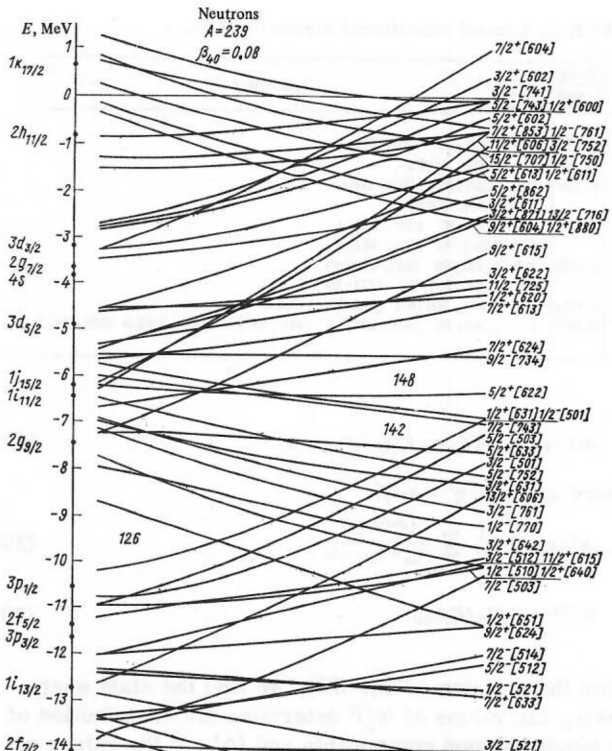

FIG. 3.

In Figs. 1–8, we give the fragments of the schemes of the single-particle levels calculated in Refs. 12 and 13 for the zones $A = 229$, 239, 247, 255 for near-equilibrium β_{40} values and in the range of β_{20} values in which the corresponding equilibrium values occur. In these figures, each level is characterized by the quantum numbers $K^\pi[Nn_z\Lambda\Sigma]$, where K is the projection of the total angular momentum of the nucleon onto the symmetry axis of the nucleus; π is the parity; $[Nn_z\Lambda\Sigma]$ are the asymptotic Nilsson quantum numbers. The indices used above: s (for neutrons), r (for protons), and q (for neutrons and protons) denote these quantum numbers. The single-particle energies are measured from the binding energies of the neutron, B_n, and the proton, B_p.

In all our calculations, we took into account the neutron levels, $E(s)$, and proton levels, $E(r)$, of the single-particle basis lying in the following intervals: $E(s(N=4)) \leqslant E(s) \leqslant 5$ MeV, $E(r(N=3)) \leqslant E(r) \leqslant 5$ MeV. The number of allowed-for levels increases with increasing A (see Table 6).

The results of the calculations of the equilibrium values of β_{20} and β_{40}, Q_{20} and Q_{40} (Ref. 22) and the corresponding experimental data[23,24] are given in Table 4. The calculations were made by the method proposed in Ref. 25.

Let us now compare the theoretical and experimental multipole moments since the values of the parameters

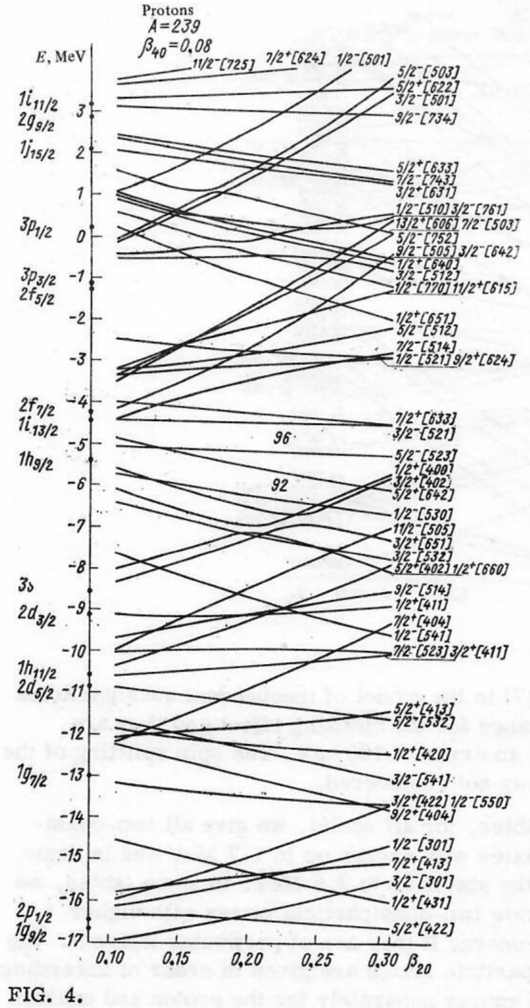

FIG. 4.

of the equilibrium deformations vary strongly depending on the experiment in which they were obtained and how the experiment was evaluated. For example, for ^{238}U the $\beta_{20}^{\text{equil}}$ values are as follows[24]: 0.283 ± 0.008; 0.27 ± 0.01; 0.22 ± 0.01. For β_{40} the values found are 0.059 ± 0.029, $0.017^{+0.015}_{-0.030}$, and 0.06 ± 0.01. The experimental data were obtained from study of the Coulomb excitation and the (p, p') and (α, α') reactions, respectively. Because of this, we regard it as more consistent to compare the values of Q_{20} and Q_{40}. The experimental data are taken from Ref. 23.

The calculated values of the correlation functions and the chemical potentials for the ground states of the neutron and proton systems are given in Table 5. These quantities may be helpful when one is estimating different nuclear characteristics.

All the parameters used to calculate the energies and wave functions of the two-quasiparticle and single-phonon states of even–even nuclei in the region $224 \leq A \leq 260$ are given in Tables 3 and 6. An increase in the number of zones for the nuclei of this region improves the description of the low-lying levels of the nuclei near the edges of these zones. For the groups of nuclei we adopted averaged values of β_{20}^0 and β_{40}^0 on the basis of the experimental and calculated values given in Table 4. With allowance for anharmonicity, the spread of the values of the constants is appreciably reduced. In Table 6 we give the nuclei for which the calculations were made with allowance for the parameters given in Table 6.

The above parameters were used in Refs. 12 and 13 to calculate nonrotational states of nuclei with an odd number of neutrons or with an odd number of protons. A satisfactory description was obtained for the energies and structure of the low-lying nonrotational states of odd deformed nuclei in the region $224 < A < 260$.

Let us now describe tables of the type Table 7, in which we give the results of calculations of the energies and structure of the two-quasiparticle states, the first single-phonon states with $K^\pi = 2^+, 0^-, 1^-$ and 2^-, and the corresponding experimental data.

In the upper part of the table, we give the two-quasiparticle proton and neutron states and the configurations of the two-quasiparticle states (q_1, q_2), F denoting the level of the Fermi surface (the last filled level for the ground state in the model of independent particles), $F+1$, $F+2$, $F+3$ denoting the first, second, third, etc., particle levels and $F-1$, $F-2$, $F-3$, denoting the first, second, third, etc., hole levels. The values of K^π in the first row correspond to a state with projection $\Sigma = 0$ of the total spin, which, in accordance with Gallagher's rule, has the least energy; those in the

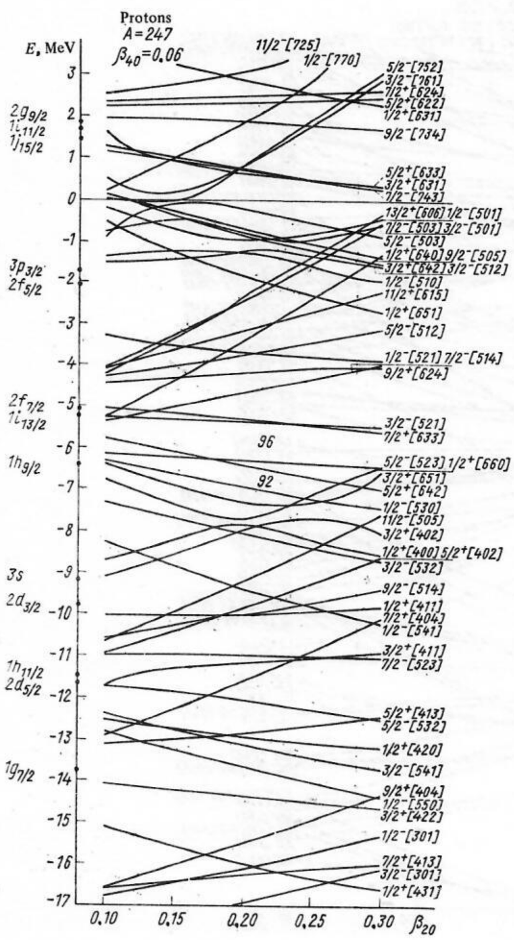

FIG. 5.

TABLE 4.

Nucleus	β_{20}^{theor}	β_{40}^{theor}	Q_{20}^{theor}, 10^{-24} cm^2	Q_{40}^{exp}, 10^{-24} cm^2	Q_{40}^{theor}, 10^{-48} cm^4	Q_{40}^{exp}, 10^{-48} cm^4
^{228}Th	0.15	0.07	7.0		2.5	
^{230}Th	0.16	0.07	7.6	9.0±0.06	2.6	2.58±0.35
^{232}Th	0.17	0.08	8.3	9.62±0.05	2.7	2.87±0.33
^{232}U	0.17	0.08	8.5	—	2.8	—
^{234}U	0.18	0.08	9.1	10.47±0.05	2.9	3.30±0.45
^{236}U	0.19	0.08	9.8	10.80±0.07	3.0	3.07±0.48
^{238}U	0.20	0.08	10.4	11.12±0.07	3.2	1.96±0.55
^{238}Pu	0.21	0.08	10.7	11.27±0.08	3.3	3.26±0.62
^{240}Pu	0.22	0.08	11.3	11.58±0.08	3.4	2.70±0.58
^{244}Cm	0.24	0.07	12.4	12.11±0.09	3.8	$0.0^{+1.18}_{-0.0}$
^{246}Cm	0.24	0.065	12.9	12.25±0.09	3.2	$0.0^{+1.18}_{-0.0}$
^{248}Cm	0.25	0.05	13.6	12.28±0.09	3.3	$0.0^{+1.4}_{-0.0}$
^{248}Cf	0.25	0.05	13.9	—	3.4	—
^{250}Cf	0.25	0.04	13.8	—	2.7	—
^{252}Cf	0.25	0.03	13.7	12.9±0.4	2.7	—
^{254}Fm	0.26	0.035	14.6	—	2.9	—
^{256}Fm	0.26	0.025	14.3	—	2.1	—

second row correspond to the state with $\Sigma=1$. In the cases when $K=0$ for one of the states of the doublet, Gallagher's rule may be broken, according to Ref. 26, so that a state with $K\neq 0$ may have a lower energy and the energy of the spin splitting is small. In the table we give the experimental and calculated energies of the two-quasiparticle states. The energies of the two-quasiparticle states are calculated in accordance with Eqs.

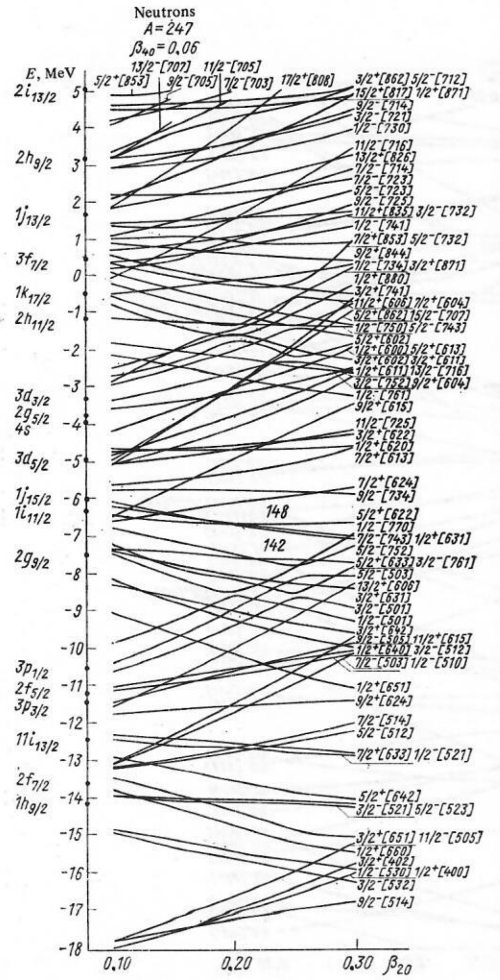

FIG. 6.

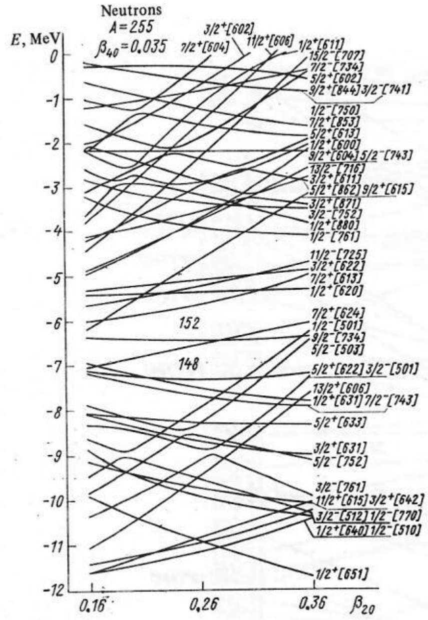

FIG. 7.

(16) and (17) in the model of independent quasiparticles with allowance for the blocking effect and they are given with an error of 100 keV. The spin splitting of the doublets was not considered.

In the tables, for all nuclei, we give all two-quasiparticle states with energy up to 1.7 MeV and in some cases all the states up to 2.5 MeV. In some tables, we give separate two-quasiparticle states with higher excitation energy if they are of particular interest. The two-quasiparticle states are given in order of ascending calculated energy separately for the proton and neutron systems.

It should be borne in mind that some states with energy greater than 2 MeV are not two-quasiparticle but con-

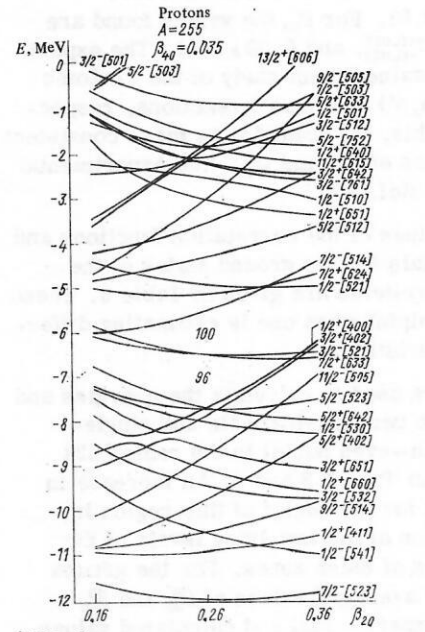

FIG. 8.

TABLE 5. Correlation functions and chemical potentials for ground states of neutron (N) and proton (Z) systems.

A zone	Neutron system			Proton system			Parameters of equilibrium deformations	
	N	C_n	λ_n	Z	C_p	λ_p	β_{20}^0	β_{40}^0
229	138 140 142	0.71 0.70 0.69	—7.01 —6.67 —6.30	90 92	0.91 0.82	—5.16 —4.68	0.19	0.10
239	142 144 146	0.63 0.65 0.65	—7.11 —6.74 —6.42	92 94	0.77 0.74	—5.88 —5.41	0.22	0.08
247	148 150 152	0.51 0.51 0.57	—6.06 —5.65 —5.28	96 98	0.51 0.56	—5.93 —5.40	0.23	0.06
255	152 154 156	0.63 0.70 0.75	—6.08 —5.72 —5.42	98 100 102 104	0.79 0.74 0.78 0.81	—6.41 —5.92 —5.43 —5.00	0.26	0.035

tain a mixture of two or more two-quasiparticle components. This is a manifestation of the incipient process of fragmentation of the two-quasiparticle state over several nuclear levels. However, in this case we ascribe the level to the two-quasiparticle component which must be the greatest. The study of this phenomenon is of independent interest, and it is particularly important to take it into account when one is investigating highly excited states of nuclei.

The states with $K^\pi = 0^+, 2^+, 0^-, 1^-$, and 2^- are indicated by the letter c. This means that these levels in tables of the type of Table 7 cannot be taken into account in the analysis of the experimental data because, as the result of the presence of the quadrupole and octupole residual interactions in the even–even nuclei, there are no pure two-quasiparticle states with these K^π values. The energies of 2^+c, 0^-c, 1^-c, and 2^-c states given in the tables are only the first, second, etc., poles of the secular equation (20). The experimental levels with the given K^π correspond to the quadrupole

TABLE 7. Two-quasiparticle and single-phonon states of ^{228}Th.

Two-quasiparticle proton states					Two-quasiparticle neutron states				
Configuration		K^π	Energy, MeV		Configuration		K^π	Energy, MeV	
			Experiment	Calculation				Experiment	Calculation
F 651↑	$F+1$ 530↑	1^-c 2^-c	—	1.7	F 752↑	$F+1$ 631↑	1^-c 4^-	—	1.0
$F-1$ 532↓	$F+1$ 530↑	2^+c 1^+	—	1.9	F 752↑	$F+2$ 633↓	5^- 0^-c	—	1.2
$F+1$ 530↑	$F+2$ 642↑	2^-c 3^-c	—	2.1	$F+1$ 631↑	$F+2$ 633↓	4^+ 1^+	—	1.4
F 651↑	$F+2$ 642↑	1^+ 4^+	—	2.2	$F-1$ 761↑	$F+1$ 631↑	3^-c 0^-c	—	1.7
$F-2$ 400↑	$F+1$ 530↑	1^-c 0^-c	—	2.2	$F-1$ 761↑	F 752↓	1^+ 4^+	—	1;7
$F-1$ 532↓	F 651↑	3^-c 0^-c	—	2.2	$F-1$ 761↑	$F+2$ 633↓	4^- 1^-c	—	1.8
$F-1$ 532↓	$F+2$ 642↑	4^- 1^-c	—	2.3	F 852↑	$F+3$ 743↑	1^+ 6^+	—	1.9
$F-3$ 402↓	$F+1$ 530↑	2^-c 1^-c	—	2.4	$F-2$ 501↓	$F+1$ 631↑	2^-c 1^-c	—	2.0

Single-phonon states

K^π	Energy, MeV		$B(E\lambda)_{s.p.u.}$		Structure, %		
	Experiment	Calculation	Experiment	Calculation			
0^-	0.328	0.3	—	28.0	nn633↓ 752↑ 49 nn631↓ 770↑ 5	nn631↑ 761↑ 6 pp651↑ 521↑ 4	pp400↑ 530↑ 5 nn642↓ 761↑ 2
1^-	—	0.7	—	27.6	nn752↑ 631↑ 28 nn752↑ 642↓ 5	nn743↑ 633↓ 8 pp651↑ 530↑ 4	nn633↓ 761↑ 5 nn633↓ 512↓ 3
2^+	0.977	0,9	—	4.5	nn752↑ 770↑ 13 nn743↑ 761↑ 10	nn631↑ 631↓ 11 pp532↓ 530↑ 6	nn633↓ 631↓ 11 nn503↓ 501↓ 5
2^-	1.123	1.1	—	12.0	nn743↑ 631↑ 14 nn743↑ 642↓ 7	pp642↑ 530↑ 9 nn633↓ 770↑ 5	nn752↑ 640↑ 8 pp651↑ 530↑ 5
3^-	—	1.8	—	0.005	nn631↑ 761↑ 100	— —	— —

and octupole vibrational states found from the solution of Eq. (20).

In the lower part of tables of the type of Table 7, we give the first quadrupole states with $K^\pi = 2^+$ and the

TABLE 6. Parameters used to calculate the energies and wave functions of two-quasiparticle and single-phonon states.

A zone	Deformation parameters		Number of single-particle levels		Pairing constants		Constants of quadrupole and octupole interactions						Nuclei
							$\varkappa^{(2)}$, keV/F^4		$\varkappa^{(3)} \cdot 10^2$ keV/F^6				
	β_{20}^0	β_{40}^0	n_N	n_Z	G_N, MeV	G_Z, MeV	$K^\pi = 0+$	$K^\pi = 2+$	$K^\pi = 0-$	$K^\pi = 1-$	$K^\pi = 2-$	$K^\pi = 3-$	
229	0.19	0.10	91	65	0.084	0.126	0.80	0.91	1.34	1.32	1.55	1.34	^{228}Th^{230}Th ^{232}Th^{232}U
239	0.22	0.08	96	68	0.082	0.116	0.73	0.85	1.24	1.16	1.36	1.20	^{234}U^{236}U ^{238}U^{238}Pu ^{240}Pu
247	0,23	0.06	101	70	0.080	0.113	0.73	0.83	1.08	1.00	1.14	1.10	^{244}Cm^{246}Cm ^{248}Cm^{248}Cf
255	0.26	0.035	105	75	0.076	0.108	0.71	0,79	0.94	0.95	0.98	0.94	^{250}Cf^{252}Cf ^{254}Fm^{256}Fm ^{254}102^{260}Ku

TABLE 8. Two-quasiparticle and single-phonon states of ^{230}Th.

Two-quasiparticle proton states					Two-quasiparticle neutron states				
Configuration		K^π	Energy, MeV		Configuration		K^π	Energy, MeV	
			Experiment	Calculation				Experiment	Calculation
F 651↑	$F+1$ 530↑	1^-c 2^-c	—	1.7	F 631↑	$F+1$ 633↓	4^+ 1^+	—	1.0
$F-1$ 532↓	$F+1$ 530↑	2^+c 1^+	—	1.9	$F-1$ 752↑	$F+1$ 633↓	5^- 0^-c	—	1.2
$F+1$ 530↑	$F+2$ 642↑	2^-c 3^-c	—	2.1	$F-1$ 752↑	F 631↑	1^-c 4^-	—	1.4
F 651↑	$F+2$ 642↑	1^+ 4^+	—	2.2	F 631↑	$F+2$ 743↑	2^-c 5^-	—	1.6
$F-2$ 400↑	$F+1$ 530↑	1^-c 0^-c	—	2.2	$F+1$ 633↓	$F+2$ 743↑	6^- 1^-c	—	1.7
$F-1$ 532↓	F 651↑	3^-c 0^-c	—	2.2	$F-1$ 752↑	$F+2$ 743↑	1^+ 6^+	—	1.7
$F-1$ 532↓	$F+2$ 642↑	4^- 1^-c	—	2.3	F 631↑	$F+3$ 631↓	2^+c 1^+	—	1.7
$F-3$ 402↓	$F+1$ 530↑	2^-c 1^-c	—	2.4	$F+1$ 633↓	$F+3$ 631↓	2^+c 3^+	—	1.8

Single-phonon states

K^π	Energy, MeV: Experiment	Energy, MeV: Calculation	$B(E\lambda)_{s.p.u.}$: Experiment	$B(E\lambda)_{s.p.u.}$: Calculation	Structure, %		
0^-	0.508	0.5	29±3	20.0	nn633↓ 752↑ 54 pp651↑ 521↑ 4	pp400↑ 530↑ 5 nn631↑ 761↑ 3	nn631↓ 770↑ $\underline{4}$ nn624↓ 743↑ 2
2^+	0.782	0.8	2.9±0.3	4.4	nn633↓ 631↓ 26 pp532↓ 530↑ $\underline{5}$	nn631↑ 631↓ $\underline{20}$ nn752↑ 770↑ $\underline{4}$	nn743↑ 761↑ $\underline{8}$ nn734↑ 752↑ $\underline{3}$
1^-	0.954	1.0	23±3	16.0	nn743↑ 633↓ 29 nn633↓ 761↑ $\underline{3}$	nn752↑ 631↓ 25 nn512↓ 631↓ $\underline{1}$	pp651↑ 530↑ 4 nn752↑ 642↓ 1
2^-	1.079	1.1	—	11.7	nn743↑ 631↑ 29 nn734↑ 633↓ 5	pp642↑ 530↑ 8 pp651↑ 530↑ $\underline{4}$	nn743↑ 642↓ 6 nn752↑ 631↓ $\underline{3}$
3^-	—	1.9	—	0.08	nn631↓ 752↑ $\underline{98}$	pp642↑ 530↑ $\underline{1}$	— —

first octupole states with $K^\pi = 0^-, 1^-$, and 2^-. In the tables we give the experimental and calculated state energies, which are arranged in ascending order of the calculated energies. The values of $B(E\lambda)$ were calculated with the effective-charge values $e_{eff}^{(2)} = 0$, $e_{eff}^{(3)} = 0.2$. In the tables, we give the values of $B(E\lambda, 0^+0_g \to I^\pi K)$ in single-particle units ($B(E2)_{s.p} = 0.3A^{4/3}e^2F^4$, $B(E3)_{s.p} = 0.42A^2E^2F_6$), where $I = 2$, $K = 0$, 2 for transitions to quadrupole states and $I = 3$, $K = 0$, 1, 2, 3 for transitions to octupole states.

In the tables, for each single-phonon state, we have given the six largest two-quasiparticle components, each of which exceeds 1%. The components are arranged in the order in which their values decrease. We use *nn* and *pp* for the neutron and proton two-quasiparticle components and underline the values of the components for which the sign of Ψ is negative [see (18) and (23)].

References to the work from which the experimental data in tables of the type of Table 7 have been taken are given in the text in the discussion of the level schemes. The values of the energy and $B(E\lambda)$ for the states whose interpretation is not sufficiently unambiguous are given in brackets.

4. ISOTOPES OF THORIUM

The experimentally best studied isotopes of thorium are ^{228}Th, ^{230}Th, ^{232}Th. Experimental information on levels up to energies ~2 MeV of ^{228}Th is obtained from β^- decay of ^{228}Ac and also from electron capture in ^{228}Pa, which have decay energies greater than 2 MeV. Electron capture in ^{230}Pa gives the excitation spectrum of ^{230}Th up to ~1 MeV. It is not possible to obtain information about the levels of ^{230}Th and ^{232}Th from β^- decay since the isotope ^{230}Ac has a lifetime shorter than 1 min, and the isotope ^{232}Ac has not been discovered experimentally. The energy of electron capture in ^{232}Pa is less than 0.5 MeV, and this prevents its use for obtaining information about excited states of ^{232}Th. Excited states of ^{228}Th, ^{230}Th, and ^{232}Th are observed in the α decay of the long-lived uranium isotopes ^{232}U, ^{234}U, and ^{236}U. Experimental information on the excitation spectra of ^{228}Th, ^{230}Th, and ^{232}Th obtained from these processes is given in Ref. 27 and systematized in Refs. 1–3, 28.

In recent years, investigations have been made of the excitation spectra of thorium isotopes by means of inelastic scattering and Coulomb excitation,[29,30] transfer reactions,[31–33] and also (n,γ) reactions.[34]

The results of calculations of the nonrotational states of ^{228}Th, ^{230}Th, and ^{232}Th and the corresponding adequately identified experimental data are given in Tables 7–9.

TABLE 9. Two-quasiparticle and single-phonon states of ^{232}Th.

Two-quasiparticle proton states					Two-quasiparticle neutron states				
Configuration		K^π	Energy, MeV		Configuration		K^π	Energy, MeV	
			Experiment	Calculation				Experiment	Calculation
F 651↑	$F+1$ 530↑	1^-c 2^-c	—	1.7	F 633↓	$F+1$ 743↑	6^- 1^-c	—	1.2
$F-1$ 532↓	$F+1$ 530↑	2^+c 1^+	—	1.9	F 633↓	$F+2$ 631↓	2^+c 3^+	—	1.3
$F+1$ 530↑	$F+2$ 642↑	2^-c 3^-c	—	2.1	$F-1$ 631↑	$F+1$ 743↑	2^-c 5^-	—	1.5
F 651↑	$F+2$ 642↑	1^+ 4^+	—	2.2	$F-1$ 631↑	$F+2$ 631↓	2^+c 1^+	—	1.5
$F-2$ 400↑	$F+1$ 530↑	1^-c 0^-c	—	2.2	$F-2$ 752↑	$F+1$ 743↑	1^+ 6^+	—	1.6
$F-1$ 532↓	F 651↑	3^-c 0^-c	—	2.2	$F-2$ 752↑	$F+2$ 631↓	3^- 2^-c	—	1.7
$F-1$ 532↓	$F+2$ 642↑	4^- 1^-c	—	2.3	$F+1$ 743↑	$F+2$ 631↓	4^- 3^-c	—	1.7
$F-3$ 402↓	$F+1$ 530↑	2^-c 1^-c	—	2.4	$F-1$ 631↑	F 633↓	4^+ 1^+	—	1.7

Single-phonon states

K^π	Energy, MeV: Experiment	Energy, MeV: Calculation	$B(E\lambda)_{s.p.u.}$: Experiment	$B(E\lambda)_{s.p.u.}$: Calculation	Structure, %		
2^+	0.786	0.8	2.9±0.2	3.4	nn633↓ 631↓ 39 pp532↓ 530↑ $\underline{4}$	nn631↑ 631↓ $\underline{21}$ nn734↑ 752↑ $\underline{3}$	nn743↑ 761↑ $\underline{5}$ pp402↓ 660↑ $\underline{2}$
0^-	0.713	0.9	20±2	11.0	nn633↓ 752↑ 37 pp651↑ 521↑ 5	nn624↓ 743↑ 12 nn631↓ 501↓ $\underline{5}$	pp660↑ 530↑ 7 nn622↑ 752↑ 3
2^-	—	1.0	—	12.0	nn743↑ 631↑ 32 nn743↑ 642↓ 4	nn734↑ 633↓ 10 pp651↑ 530↑ $\underline{3}$	pp642↑ 530↑ 7 nn752↑ 631↓ $\underline{3}$
1^-	1.045	1.1	11.5±2.3	11.2	nn743↑ 633↓ 61 nn743↑ 622↑ 3	nn752↑ 631↑ 4 pp523↑ 402↓ 1	pp651↑ 530↑ 3 nn734↑ 624↓ 1
3^-	—	1.7	—	0.04	nn743↑ 631↓ $\underline{99}$	— — —	— — —

TABLE 10. Two-quasiparticle and single-phonon states of ^{232}U.

Two-quasiparticle proton states					Two-quasiparticle neutron states				
Configuration		K^π	Energy, MeV		Configuration		K^π	Energy, MeV	
			Experiment	Calculation				Experiment	Calculation
F 530↑	$F+1$ 642↑	2^-c 3^-c	—	1.6	F 631↑	$F+1$ 633↓	4^+ 1^+	—	1.0
F 530↑	$F+2$ 523↓	3^+ 2^+c	—	2.0	$F-1$ 752↑	$F+1$ 633↓	5^- 0^-c	—	1.2
$F-1$ 651↑	$F+1$ 642↑	1^+ 4^+	—	2.0	$F-1$ 752↑	F 631↑	1^-c 4^-	—	1.4
$F-2$ 532↓	$F+1$ 642↑	4^- 1^-c	—	2.2	F 631↑	$F+2$ 743↑	2^-c 5^-	—	1.6
$F+1$ 642↑	$F+2$ 523↓	5^- 0^-c	—	2.3	$F+1$ 633↓	$F+2$ 743↑	6^- 1^-c	—	1.7
$F-1$ 651↑	$F+2$ 523↓	4^- 1^-c	—	2.4	$F-1$ 752↑	$F+2$ 743↑	1^+ 6^+	—	1.7
F 530↑	$F+3$ 521↑	1^+ 2^+c	—	2.5	F 631↑	$F+3$ 631↓	2^+c 1^+	—	1.7

Single-phonon states

K^π	Energy, MeV		$B(E\lambda)_{s.p.u.}$		Structure, %		
	Experiment	Calculation	Experiment	Calculation			
0^-	0.564	0.5	—	16.0	nn633↓ 752↑ 56 nn631↑ 761↑ 3	pp651↑ 521↑ 6 nn624↓ 743↑ 2	nn631↓ 501↓ 4 pp660↑ 530↑ 2
2^+	0.867	0.9	—	3.0	nn633↓ 631↓ 30 nn752↑ 501↓ 4	nn631↑ 631↓ 23 nn734↓ 752↑ 3	nn743↑ 761↑ 8 pp532↓ 530↑ 2
2^-	1.019	1.0	—	11.4	nn743↑ 631↑ 28 nn734↑ 633↓ 5	pp642↑ 530↑ 13 nn752↑ 631↓ 3	nn743↑ 642↓ 6 nn631↓ 761↑ 2
1^-	—	1.1	—	13.4	nn743↑ 633↓ 30 nn633↓ 761↑ 3	nn752↑ 631↑ 27 pp651↑ 530↑ 2	pp642↑ 521↑ 3 nn752↑ 642↓ 1
3^-	—	1.8	—	0.3	pp642↑ 530↑ 97	nn631↓ 752↑ 2	— — —

In ^{228}Th and ^{230}Th the first $K^\pi=0^-$ state has a very low energy. This leads to the appearance of appreciable two-phonon admixtures to the basic single-phonon components, as can be seen in Table 1. Therefore, the first 0^+ state in ^{228}Th has a predominant two-phonon component, and in ^{230}Th and ^{232}Th there are large admixtures of two-phonon components. It can be seen from Table 2 that the calculated energies of the first 0^+ states agree well with the experiment. The calculated $B(E2, 0_g \to I^\pi K = 2^+0)$ values for ^{230}Th and ^{232}Th, which are equal to 4 and 2.6, do not differ strongly from the experimental values 1.10 ± 0.14 and 2.9 ± 0.2.

It can be seen from Tables 7–9 that the calculated energies and $B(E\lambda)$ for the first quadrupole $K^\pi = 2^+$ and octupole states agree reasonably with the experimental data taken from Ref. 30.

An example of an octupole state with $K^\pi = 1^-$ in the thorium isotopes is the well established level 954 keV in ^{230}Th (Refs. 1–3, 28, 30); its energy and $B(E3, 0_g \to I=3,\ K=1)_{exp}$ are reproduced in the calculation (see Table 8). The experimental information about octupole states with $K^\pi = 0^-, 1^-$ in ^{232}Th are somewhat contradictory. For example, in Refs. 2–3, 28, 34 the quantum numbers $K^\pi = 0^-$ are ascribed to the level 1045 keV but in Ref. 29, in the (d, d') reaction, Else and Huizenga established states 713 keV with $K^\pi = 0^-$ and 1107 keV with $I^\pi = 3^-$. In Ref. 30, in the (α, α) reaction, McGowan *et al.* observed levels 774 keV with $K^\pi = 0^-, I = 3$ and 1106 keV with $K^\pi = 1^-$, $I = 3$.

Combined analysis of these papers suggests that the vibrational octupole state $K^\pi = 0^-$ has energy 713 keV, and a state with $K^\pi = 1^-$ lies in the range 1000–1100 keV. The corresponding states in the calculation made for ^{232}Th agree perfectly satisfactorily as regards the energy and the values of $B(E3, 0_g \to I=3, K=0,\ 1)_{exp}$ (see Table 9).

Octupole states with $K^\pi = 0^-$ in the radium isotopes and the light isotopes of thorium in the range 200–300 keV have long been known.[35] More recently, these states, and also the first states with $K^\pi = 0^-$ in the isotopes of uranium, plutonium, and the heavier actinides were investigated in many experimental and theoretical studies.[10,11,29,30,36–39] The very strong lowering of the energies of the first 0^- states in the light isotopes of thorium and uranium was explained and then studied in more detail in Ref. 10. In Ref. 39, these states were calculated with allowance for the interaction of the quasiparticles with the phonons and a satisfactory description was obtained for the energies of the first 0^- states. Calculations of the single-phonon states for ^{228}Th, ^{230}Th, ^{232}Th, ^{232}U (see Tables 7–10) were taken from Ref. 11. As can be seen from the tables, in the single-phonon approximation one can correctly describe the known energies and the $B(E3, 0_g \to I=3,\ K=0)_{exp}$

TABLE 11. Two-quasiparticle and single-phonon states of ^{234}U.

Two-quasiparticle proton states					Two-quasiparticle neutron states				
Configuration		K^π	Energy, MeV		Configuration		K^π	Energy, MeV	
			Experiment	Calculation				Experiment	Calculation
F 530↑	$F+1$ 642↑	2^-c 3^-	— 1.723	1.4	F 633↓	$F+1$ 743↑	6^- 1^-c	1,421	1.3
F 530↑	$F+2$ 523↓	3^+ 2^+c	—	1.7	F 633↓	$F+2$ 631↓	2^+c 3^+	 1.496	1.3
$F-1$ 651↑	$F+1$ 642↑	1^+ 4^+	 1.724	1.8	F 633↓	$F+3$ 622↑	5^+ 0^+c	1,552	1.4
$F+1$ 642↑	$F+2$ 523↓	5^- 0^-c	—	1.9	$F-1$ 752↑	$F+1$ 743↑	1^+ 6^+	—	1.5
$F-1$ 651↑	$F+2$ 523↓	4^- 1^-c	—	2.0	$F-1$ 752↑	$F+2$ 631↓	3^- 2^-c	—	1,6
$F-2$ 400↑	$F+2$ 523↓	3^+ 2^+c	—	2.1	$F-1$ 752↑	$F+3$ 622↑	5^- 0^-c	—	1.7
$F-3$ 532↓	$F+1$ 642↑	4^- 1^-c	—	2,2	$F-2$ 631↑	$F+1$ 743↑	2^-c 5^-	— 1.694	1.8
$F-1$ 651↑	F 530↑	1^-c 2^-c	—	2,2	$F-3$ 501↓	$F+1$ 743↑	4^+ 3^+	1,884 1,956	2.0 —

Single-phonon states

K^π	Energy, MeV		$B(E\lambda)_{s.p.u.}$		Structure, %		
	Experiment	Calculation	Experiment	Calculation			
0^-	0,786	0.7	26±3	20.3	nn622↑ 752↑ 21 pp523↓ 642↑ 5	nn633↓ 752↑ 16 nn624↓ 743↑ 4	pp521↑ 651↑ 9 pp530↑ 400↑ 4
2^+	0.927	0.9	2.9± 0,3	4.5	nn633↓ 631↓ 43 pp642↑ 660↑ 3	nn631↑ 631↓ 19 nn734↑ 752↑ 3	nn743↑ 761↑ 6 nn503↓ 501↓ 2
2^-	0.989	0.9	9.5± 2,3	6.9	pp642↑ 530↑ 68 nn734↑ 633↓ 1	nn743↑ 631↑ 14 nn631↓ 761↑ 1	nn752↑ 631↓ 3 pp530↑ 651↑ 1
1^-	(1,436)	1.0	—	8.9	nn743↑ 633↓ 73 pp651↑ 530↑ 2	nn743↑ 622↑ 5 pp523↓ 402↓ 1	pp642↑ 521↑ 2 nn752↑ 631↑ 1

TABLE 12. Two-quasiparticle and single-phonon states of ^{236}U.

Two-quasiparticle proton states					Two-quasiparticle neutron states				
Configuration		K^π	Energy, MeV: Experiment	Energy, MeV: Calculation	Configuration		K^π	Energy, MeV: Experiment	Energy, MeV: Calculation
F 530↑	$F+1$ 642↑	2^-c 3^-c	—	1.4	F 743↑	$F+1$ 631↓	4^- 3^-c	1.054	1.0
F 530↑	$F+2$ 523↓	3^+ 2^+c	—	1.7	F 743↑	$F+2$ 622↑	1^-c 6^-	 1.472	1.2
$F-1$ 651↑	$F+1$ 642↑	1^+ 4^+	—	1.8	$F-1$ 633↓	$F+1$ 631↓	2^+c 3^+	—	1.6
$F+1$ 642↑	$F+2$ 523↓	5^- 0^-c	—	1.9	$F-1$ 633↓	F 743↑	6^- 1^-c	—	1.6
$F-1$ 651↑	$F+2$ 523↓	4^- 1^-c	—	2.0	$F-1$ 633↓	$F+2$ 622↑	5^+ 0^+c	—	1.6
$F-2$ 400↑	$F+2$ 523↓	3^+ 2^+c	—	2.1	F 743↑	$F+3$ 624↓	7^- 0^-c	—	1.7
$F-3$ 532↓	$F+1$ 642↑	4^- 1^-c	—	2.2	$F+1$ 631↓	$F+3$ 624↓	3^+ 4^+	—	1.8

Single-phonon states

K^π	Energy, MeV: Experiment	Energy, MeV: Calculation	$B(E\lambda)_{s.p.u.}$: Experiment	$B(E\lambda)_{s.p.u.}$: Calculation	Structure, %		
0^-	0.685	0.5	23±3	25.0	nn 622↑ 752↑ 19 pp 523↓ 642↑ 4	nn 624↓ 743↑ 19 pp 530↑ 400↑ 4	pp 521↑ 651↑ 9 nn 633↓ 752↑ 3
1^-	0.970	0.9	—	3.6	nn 743↑ 622↑ 90 pp 651↑ 530↑ 1	nn 743↑ 633↓ 2	pp 642↑ 521↑ 1
2^-	—	0.9	—	6.7	pp 642↑ 530↑ 77 nn 734↑ 633↓ 1	nn 743↑ 631↑ 5 nn 752↑ 631↓ 1	nn 734↑ 622↑ 3 nn 613↑ 501↑ 1
3^-	1.192	1.0	—	0.3	nn 743↑ 631↓ 96	pp 530↑ 642↑ 1	— — —
2^+	0.959	1.1	4.2±0.4	3.5	nn 633↓ 631↓ 44 nn 743↑ 761↑ 4	nn 631↑ 631↓ 14 pp 642↑ 660↑ 4	nn 622↑ 631↓ 5 nn 734↑ 752↑ 4

values in these nuclei. As was already noted in Ref. 11, the appearance of low 0_1^- states in isotopes with $N=136$, 138, 140 can be explained by the strong influence of the two lowest poles $nn633\downarrow 752\uparrow$ and $nn631\uparrow 761\uparrow$. These poles are situated at nearly equal energies and the corresponding matrix elements of the operator of the multipole moment with $\lambda\mu=30$ have large values.

In ^{228}Th, one can take as well established the octupole state 1123 keV with $K^\pi=2^-$.[1–3,27,28] In the electron-capture reaction in ^{230}Pa (Refs. 1–3, 28) one observes a 2^- level at 1080 keV in ^{230}Th which does not occur in the rotational band based on the octupole state with $K^\pi=1^-$. As can be seen from Tables 7 and 8, the energies of these levels are reproduced well in the calculations. There is no experimental information about states with $K^\pi=3^-$ in the thorium isotopes.

5. ISOTOPES OF URANIUM

We here discuss the nonrotational states of ^{232}U, ^{234}U, ^{236}U, ^{238}U. The uranium isotopes have been studied comparatively well in experiments. The β^- decay of ^{232}Pa was studied in Refs. 40 and 41 and electron capture in ^{232}Np in Refs. 40, 42, and 43. Experimental information on the excitation spectrum of ^{232}U up to 1 MeV obtained from these processes and also from the α decay of ^{236}Pu (Refs. 44 and 45) is systematized in Refs. 1–3 and 28. In Ref. 31, the excited states of ^{232}U obtained from the (p,t) reaction are given. In β^- decay having energy 1.4 MeV the bases and some levels of rotational bands based on states with $K^\pi=0^+, 2^+, 0^-, 2^-$ have been established. Data from electron capture in ^{232}Np, the α decay of ^{236}Pu, and the (p,t) reaction confirm the energies of these states.

The results of calculations and the experimental data for ^{232}U are given in Tables 2 (0^+ states) and 10. The theoretical energies of the first quadrupole and octupole states agree well with the experimentally known energies. As we have already noted in Sec. 4, the energy and structure of the first 0^- state of ^{232}U is determined, as in the case of the thorium isotopes, by the influence of the first pole $nn633\downarrow 752\uparrow$.

The excitation spectrum of ^{234}U has been obtained by studying the β^- decay of the metastable state $T_{1/2}=1.17$ min of ^{234}Pa (Refs. 46–49), the β decay of the ground state of ^{234}Pa (Refs. 38, 50, 51), electron capture in ^{234}Np (Refs. 47 and 52), and also the α decay of ^{238}Pu (Refs. 53–56). The experimental data obtained in these processes and also in the (d,p) and (d,t) reactions[57] were systematized in Refs. 1–3 and 28. In recent years, ^{234}U has been investigated in Coulomb excitation,[30] and in the (p,t) (Ref. 31) and (d,d') (Ref. 58) reactions.

Analysis of the experimental data on ^{234}U has estab-

TABLE 13. Two-quasiparticle and single-phonon states of ^{238}U.

Two-quasiparticle proton states					Two-quasiparticle neutron states				
Configuration		K^π	Energy, MeV: Experiment	Energy, MeV: Calculation	Configuration		K^π	Energy, MeV: Experiment	Energy, MeV: Calculation
F 530↑	$F+1$ 642↑	2^-c 3^-c	—	1.4	F 631↓	$F+1$ 622↑	3^+ 2^+c	(1.06)	1.1
F 530↑	$F+2$ 523↓	3^+ 2^+c	—	1.7	$F-1$ 743↑	$F+1$ 622↑	1^-c 6^-	—	1.1
$F-1$ 651↑	$F+1$ 642↑	1^+ 4^+	—	1.8	$F-1$ 743↑	F 631↓	4^- 3^-c	—	1.2
$F+1$ 642↑	$F+2$ 523↓	5^- 0^-c	—	1.9	F 631↓	$F+2$ 624↓	3^+ 4^+	—	1.4
$F-1$ 651↑	$F+2$ 523↓	4^- 1^-c	—	2.0	$F-1$ 743↑	$F+2$ 624↓	7^- 0^-c	—	1.4
$F-2$ 400↑	$F+2$ 523↓	3^+ 2^+c	—	2.1	$F+1$ 622↑	$F+2$ 624↓	6^+ 1^+	—	1.4
$F-3$ 532↓	$F+1$ 642↑	4^- 1^-c	—	2.2	F 631↓	$F+3$ 734↑	5^- 4^-	—	1.8

Single-phonon states

K^π	Energy, MeV: Experiment	Energy, MeV: Calculation	$B(E\lambda)_{s.p.u.}$: Experiment	$B(E\lambda)_{s.p.u.}$: Calculation	Structure, %		
0^-	0.680	0.7	27±2.5	22.2	nn 624↓ 743↑ 35 pp 523↓ 642↑ 5	pp 521↑ 651↑ 9 pp 530↑ 400↑ 4	nn 622↑ 752↑ 8 pp 530↑ 660↑ 2
2^-	—	0.8	—	10.0	pp 642↑ 530↑ 61 nn 734↑ 633↓ 2	nn 734↑ 622↑ 16 nn 613↑ 501↑ 1	nn 743↑ 631↑ 2 pp 530↑ 651↑ 1
1^-	0.931	1.0	—	10.1	nn 743↑ 622↑ 74 nn 743↑ 633↓ 2	nn 734↑ 624↓ 2 pp 523↓ 402↓ 1	pp 642↑ 521↑ 2 pp 521↑ 400↑ 1
2^+	1.061	1.1	2.9±0.23	5.0	nn 633↓ 631↓ 20 nn 631↑ 631↓ 8	nn 622↑ 631↓ 13 pp 642↑ 660↑ 5	nn 622↑ 620↑ 10 nn 734↑ 752↑ 5
3^-	—	1.1	—	0.3	nn 743↑ 631↓ 90	pp 530↑ 642↑ 9	— — —

TABLE 14. Two-quasiparticle and single-phonon states of ^{238}Pu.

Two-quasiparticle proton states: Configuration		K^π	Energy, MeV: Experiment	Energy, MeV: Calculation	Two-quasiparticle neutron states: Configuration		K^π	Energy, MeV: Experiment	Energy, MeV: Calculation
F 642↑	$F+1$ 523↓	5^- 0^-c	—	1.1	F 743↑	$F+1$ 631↓	4^- 3^-c	(1.082)	1.0
$F-1$ 530↑	$F+1$ 523↓	3^+ 2^+c	—	1.8	F 743↑	$F+2$ 622↑	1^-c 6^-	—	1.2
F 642↑	$F+2$ 521↑	1^-c 4^-	—	1.8	$F-1$ 633↓	$F+1$ 631↓	2^+c 3^+	—	1.6
$F-1$ 530↑	F 642↑	2^-c 3^-c	—	2.0	$F-1$ 633↓	F 743↑	6^- 1^-c	—	1.6
$F+1$ 523↓	$F+2$ 521↑	4^+ 1^+	—	2.0	$F-1$ 633↓	$F+2$ 622↑	5^+ 0^+c	—	1.6
$F-1$ 530↑	$F+2$ 521↑	1^+ 4^+	—	2.0	F 743↑	$F+3$ 624↓	7^- 0^-c	—	1.7
F 642↑	$F+3$ 633↑	1^+ 6^+	—	2.1	$F+1$ 631↓	$F+3$ 624↓	3^+ 4^+	—	1.8

Single-phonon states

K^π	Energy, MeV: Experiment	Energy, MeV: Calculation	$B(E\lambda)_{s.p.u.}$: Experiment	$B(E\lambda)_{s.p.u.}$: Calculation	Structure, %		
0^-	0.605	0.5	30±5	31.8	nn 624↓ 743↑ 16 pp 521↑ 651↑ 10	nn 622↑ 752↑ 16 nn 633↓ 752↑ 3	pp 523↓ 642↑ 12 pp 512↑ 642↑ 3
1^-	0.963	0.9	—	3.5	nn 743↑ 622↑ 89	pp 642↑ 521↑ 4	nn 743↑ 633↓ 2
3^-	—	1.0	—	0.3	nn 743↑ 631↓ 99		
2^+	1.028	1.1	—	3.2	nn 633↓ 631↓ 46 nn 743↑ 761↑ 4	nn 631↑ 631↓ 14 nn 734↑ 752↑ 4	nn 622↑ 631↓ 6 pp 633↑ 651↑ 2
2^-	1.310	1.2	—	11.8	nn 743↑ 631↓ 23 nn 752↑ 631↓ 5	Pp 642↑ 530↑ 19 n 734↑ 633↓ 4	nn 734↑ 622↑ 13 nn 613↑ 501↑ 2

lished vibrational states with $K^\pi = 0^+, 2^+, 0^-, 1^-, 2^-$ and also some two-quasiparticle states. In Table 11, we give the results of calculations of the nonrotational states of ^{234}U and the corresponding experimental data. The calculations reproduce well the quantum numbers of vibrational states. The first two 0^+ states whose structure is given in Table 2 are mainly single-phonon states. For the first 0^+ state, the calculated value $B(E2) = 3.4$ agrees with the experimental value 2.3 ± 0.3. In ^{234}U, study of the (d, p) and (d, t) reactions[57] and the β^- decay of ^{234}Pa (Ref. 38) has led to the experimental discovery of eight two-quasiparticle states whose energies are correctly predicted by theory.[10]

The excitation spectrum of ^{236}U was studied in the β^- decay of ^{236}Pa (Refs. 59 and 60), in electron capture in the metastable state with $T_{1/2} = 22.5$ h of ^{236}Np (Ref. 61), and in the α decay of ^{240}Pu (Refs. 53 and 62). The resulting experimental data were systematized in Refs. 1–3 and 28. The nucleus ^{236}U was also studied in the (t, p) (Ref. 33) and (p, t) (Ref. 31) reactions, in Coulomb (α, α') excitation (Ref. 30), and in the (n, γ) (Refs. 63 and 64) and (d, d') (Ref. 65) reactions. The determined energies of the first quadrupole and octupole states and the $B(E\lambda)$ values are well reproduced in the calculations (Table 12). The structure of the 0^+ states is given in Table 12; the two-phonon components constitute 15–25%. In Ref. 66, in a study of the (d, p) reaction, two-quasiparticle states whose energies and structure correspond to the results of the calculations were found (see Table 12).

The excitation spectrum of ^{238}U was obtained in the β^- decay of ^{238}Pa (Refs. 59 and 61), which has an energy of 4 MeV. One cannot use electron capture in ^{238}Np to obtain information about the excited states of ^{238}U since the energy of this process is 140 keV. In Refs. 54 and 67, a study was made of the α decay of ^{242}Pu. These data, and also the results obtained from Coulomb excitation (Refs. 68 and 69) and the (n, n') (Refs. 70 and 71) and (d, d') (Ref. 72) reactions are systematized in Refs. 1–3 and 28. Excited states of ^{238}U were also studied in the (α, α) (Ref. 30), (t, p) (Ref. 33), (d, d') (Ref. 29), and (n, n') (Ref. 34) reactions.

The results of the calculations and the experimental data for ^{238}U are given in Tables 13 and 2. There are well established levels with $K^\pi = 0^+, 2^+, 0^-, 1^-$ whose energies and existing $B(E\lambda)$ values are reproduced perfectly satisfactorily in the calculations. The two-phonon components for these states do not exceed 10%. In Coulomb excitation one observes two levels with $K^\pi = 0^+$ with nearly equal energies: 925 and 993 keV (Refs. 1–3, 68, and 69), for which the $B(E2)$ values are 0.4 ± 0.1 and 1.4 ± 0.2 (Ref. 30).

In Table 2, we give the results of calculations of the two lowest 0^+ states in ^{238}U. It can be seen from Table 2

TABLE 15. Two-quasiparticle and single-phonon states of ^{240}Pu.

Two-quasiparticle proton states: Configuration		K^π	Energy, MeV: Experiment	Energy, MeV: Calculation	Two-quasiparticle neutron states: Configuration		K^π	Energy, MeV: Experiment	Energy, MeV: Calculation
F 642↑	$F+1$ 523↓	5^- 0^-c	1.308	1.2	F 631↓	$F+1$ 622↑	3^+ 2^+c	1.031	1.1
$F-1$ 530↑	$F+1$ 523↓	3^+ 2^+c	—	1.8	$F-1$ 743↑	$F+1$ 622↑	1^-c 6^-	—	1.1
F 642↑	$F+2$ 521↑	1^-c 4^-	—	1.8	$F-1$ 743↑	F 631↓	4^- 3^-c	—	1.2
$F-1$ 530↑	F 642↑	2^-c 3^-c	—	2.0	F 631↓	$F+2$ 624↓	3^+ 4^+	—	1.4
$F+1$ 523↓	$F+2$ 521↑	4^+ 1^+	—	2.0	$F-1$ 743↑	$F+2$ 624↓	7^- 0^-c	—	1.4
$F-1$ 530↑	$F+2$ 521↑	1^+ 4^+	—	2.0	$F+1$ 622↑	$F+2$ 624↓	6^+ 1^+	—	1.4

Single-phonon states

K^π	Energy, MeV: Experiment	Energy, MeV: Calculation	$B(E\lambda)_{s.p.u.}$: Experiment	$B(E\lambda)_{s.p.u.}$: Calculation	Structure, %		
0^-	0.597	0.7	17±2.5	20,5	nn 624↑ 743↑ 33 nn 622↑ 752↑ 8	pp 523↓ 642↑ 12 pp 512↑ 642↑ 2	pp 521↑ 651↑ 9 nn 613↑ 743↑ 2
2^+	0.938	0.9	1.8±0.4	0.2	nn 622↑ 631↓ 98	— — —	— — —
1^-	—	1.0	—	9.5	nn 743↑ 622↑ 72 nn 743↑ 633↓ 2	pp 642↑ 521↑ 8 pp 523↓ 402↓ 1	nn 734↑ 624↓ 2 pp 521↑ 400↑ 1
2^-	0.959	1.0	—	13.8	nn 734↑ 622↑ 42 nn 734↑ 633↓ 4	pp 642↑ 530↑ 13 nn 613↑ 501↑ 2	nn 743↑ 631↑ 5 pp 633↑ 521↑ 2
3^-	—	1.1	—	0.3	nn 743↑ 631↓ 99	— — —	— — —
2^+	(1.559)	1.4	—	3.2	nn 633↓ 631↓ 35 nn 734↑ 752↑ 6	nn 622↑ 620↑ 10 pp 633↑ 651↑ 3	nn 631↑ 631↓ 9 pp 521↑ 530↑ 3

TABLE 16. Two-quasiparticle and single-phonon states of ^{244}Cm.

Two-quasiparticle proton states: Configuration		K^π	Energy, MeV: Experiment	Energy, MeV: Calculation	Two-quasiparticle neutron states: Configuration		K^π	Energy, MeV: Experiment	Energy, MeV: Calculation
F 523↓	$F+1$ 521↑	4^+ 1^+	—	1.3	F 622↑	$F+1$ 624↓	6^+ 1^+	1.042	1.0
F 523↓	$F+2$ 633↑	6^- 1^-c	—	1.4	$F-1$ 743↑	$F+1$ 624↓	7^- 0^-c	—	1.1
$F-1$ 642↑	$F+1$ 521↑	1^-c 4^-	—	1.6	$F-2$ 631↓	$F+1$ 624↓	3^+ 4^+	—	1.2
$F-1$ 642↑	$F+2$ 633↑	1^+ 6^+	—	1.6	F 622↑	$F+2$ 734↑	2^-c 7^-	—	1.3
$F+1$ 521↑	$F+2$ 633↑	2^-c 5^-	—	1.9	$F-1$ 743↑	$F+2$ 734↑	1^+ 8^+	—	1.4
$F-1$ 642↑	F 523↓	5^- 0^-c	—	2.0	$F-2$ 631↓	$F+2$ 734↑	5^- 4^-	—	1.4
$F-2$ 530↑	$F+1$ 521↑	1^+ 2^+c	—	2.1	$F+1$ 624↑	$F+2$ 734↑	1^-c 8^-	—	1.5
$F-2$ 530↑	$F+2$ 633↑	3^-c 4^-	—	2.1	$F-1$ 743↑	F 622↑	1^-c 6^-	—	1.6

Single-phonon states

K^π	Energy, MeV: Experiment	Energy, MeV: Calculation	$B(E\lambda)_{\text{s.p.u.}}$: Experiment	$B(E\lambda)_{\text{s.p.u.}}$: Calculation	Structure, %		
2^-	—	0.96	—	5.4	nn 734↑ 622↑ 77 nn 725↑ 624↓ 2	pp 633↑ 521↑ 4 pp 514↓ 651↑ 1	nn 734↑ 633↓ 4 nn 624↓ 501↑ 1
0^-	—	1.0	—	13.5	nn 624↓ 743↑ 51 nn 600↑ 501↓ 2	pp 402↓ 521↑ 5 pp 642↑ 512↑ 2	pp 642↑ 523↓ 3 nn 602↓ 761↑ 2
2^+	—	1.20	—	3.0	nn 622↑ 620↑ 34 pp 521↑ 530↑ 4	nn 624↓ 622↓ 17 nn 633↓ 631↓ 4	nn 734↑ 752↑ 6 pp 633↑ 402↓ 4
1^-	—	1.20	—	2.1	pp 633↑ 523↓ 74 pp 642↑ 521↑ 6	nn 734↑ 624↓ 8 — — —	nn 743↑ 622↑ 7 — — —
1^-	—	1.30	—	2.6	nn 743↑ 622↑ 29 pp 642↑ 521↑ 16	pp 633↑ 523↓ 25 pp 521↑ 400↑ 1	nn 734↑ 624↓ 23 nn 743↑ 633↓ 1
3^-	—	1.71	—	0.9	nn 743↑ 631↓ 77 nn 734↑ 631↑ 1	pp 633↑ 530↑ 15 nn 615↓ 501↑ 1	nn 725↑ 622↑ 2 nn 725↑ 633↓ 1

that they both have a complicated structure, although the main contribution to the 0_1^+ state is given by a β-vibrational phonon and that to the 0_2^+ state by the two-phonon component (301, 301).

Note that two close 0^+ levels were also observed in (p, t) reactions in ^{238}Pu (Ref. 73) and in ^{240}Pu (Ref. 31). In Ref. 32, investigations were made of 0^+ states in ^{232}Th, ^{236}Th, and ^{238}U in the (t, p) reaction and it was established that the levels 730 keV in ^{232}Th and 993 keV in ^{238}U (see Table 2) are not excited in the (t, p) reaction and that the level 920 keV in ^{236}U is excited very weakly.

The results of the experimental and theoretical investigations of the 0^+ states in these nuclei indicate that these states have a complicated nature. At the present time, there is no satisfactory unambiguous description of all the 0^+ states observed in the experiments.

6. ISOTOPES OF PLUTONIUM

We now discuss the nonrotational states of ^{238}Pu and ^{240}Pu. Experimental data on ^{238}Pu levels have been obtained from the β^- decay of ^{238}Np (Ref. 74), electron capture in ^{238}Am (Ref. 75), and α decay of ^{242}Cm (Refs. 37, 76–78), and these data have been systematized in Refs. 1–3 and 28. Excited states of ^{238}Pu have also been investigated by means of the (p, t) reaction[73] and Coulomb excitation in the (α, α') process (Ref. 31). In Table 14, we give the results of calculations of the lowest quadrupole and octupole states of ^{238}Pu and the available experimental data. It is now well established that there is a γ vibrational state with energy 1028 keV and an octupole state with $K^\pi = 0^-$ and energy 605 keV. These states are well reproduced in the calculations. The admixtures to the single-phonon components do not exceed 10%. A state with $K^\pi = 0^+$ has been observed in many investigations,[37,74–78] and in Ref. 73 it was established that there are two close 0^+ states at 945 and 1134 keV. The results of calculations with allowance for anharmonicity given in Table 2 show that the first 0^+ state is essentially a single-phonon state and that the second 0^+ state has a complicated structure with a large two-phonon component (301, 301). The energies of these states are reproduced satisfactorily.

Excited states of ^{240}Pu were investigated in the β^- decay of the metastable state $T_{1/2} = 7.4$ min of ^{240}Np (Ref. 79), in the β^- decay of the ground state of ^{240}Np (Refs. 48 and 79), in electron capture in ^{240}Am (Ref. 80), and in the α decay of ^{244}Cm (Refs. 76 and 77). In Ref. 31, the levels of ^{240}Pu were investigated by means of the (p, t) reaction and in Ref. 30 by means of Coulomb excitation in the (α, α') process. In β^- decay of the state $T_{1/2} = 7.4$ min of ^{240}Np, nonrotational states with $K^\pi = 0^-, 2^-, 0^+$ were established. In Ref. 30, the $B(E\lambda)$ values were determined for transitions to levels with $K^\pi = 2^+$ (938 keV) and $K^\pi I = 0^- 3$ (661 keV).

TABLE 17. Two-quasiparticle and single-phonon states of ^{246}Cm.

Two-quasiparticle proton states: Configuration		K^π	Energy, MeV: Experiment	Energy, MeV: Calculation	Two-quasiparticle neutron states: Configuration		K^π	Energy, MeV: Experiment	Energy, MeV: Calculation
F 523↓	$F+1$ 521↑	4^+ 1^+	—	1.3	F 624↓	$F+1$ 734↑	8^- 1^-c	—	0.8
F 523↓	$F+2$ 633↑	6^- 1^-c	—	1.4	F 624↓	$F+2$ 613↑	7^+ 0^+c	—	1.3
$F-1$ 642↑	$F+1$ 521↑	1^-c 4^-	—	1.6	$F-1$ 622↑	$F+1$ 734↑	2^-c 7^-	—	1.5
$F-1$ 642↑	$F+2$ 633↑	1^+ 6^+	—	1.6	$F+1$ 734↑	$F+2$ 613↑	1^-c 8^-	—	1.5
$F+1$ 521↑	$F+2$ 633↑	2^-c 5^-	—	1.9	$F-2$ 743↑	$F+1$ 734↑	1^+ 8^+	—	1.5
$F-1$ 642↑	F 523↓	5^- 0^-c	—	2.0	$F-3$ 631↓	$F+1$ 734↑	5^- 4^-	—	1.6
$F-2$ 530↑	$F+1$ 521↑	1^+ 2^+c	—	2.1	$F-1$ 622↑	F 624↓	6^+ 1^+	—	1.6
$F-2$ 530↑	$F+2$ 633↑	3^-c 4^-	—	2.1	F 624↓	$F+2$ 620↑	4^+ 3^+	—	1.7

Single-phonon states

K^π	Energy, MeV: Experiment	Energy, MeV: Calculation	$B(E\lambda)_{\text{s.p.u.}}$: Experiment	$B(E\lambda)_{\text{s.p.u.}}$: Calculation	Structure, %		
2^-	0.843	0.9	—	3.0	nn 734↑ 622↑ 44 nn 725↑ 613↑ 3	pp 633↑ 521↑ 16 nn 734↑ 633↓ 2	nn 725↑ 624↓ 10 nn 613↑ 501↑ 2
0^-	1.25	1.0	—	16.2	nn 624↓ 743↑ 27 pp 521↑ 402↓ 4	pp 521↑ 651↑ 6 nn 600↑ 501↓ 4	pp 523↓ 642↑ 5 nn 615↓ 734↑ 3
1^-	1.079	1.0	—	1.4	nn 734↑ 624↓ 81 nn 743↑ 622↑ 1	nn 734↑ 613↑ 5 pp 521↑ 660↑ 1	pp 642↑ 511↑ 4 — — —
2^+	1.126	1.1	(4.9±1.0)	2.9	nn 624↓ 622↓ 34 nn 725↑ 743↑ 3	nn 622↑ 620↑ 24 pp 521↑ 530↑ 3	nn 734↑ 752↑ 5 pp 523↓ 521↓ 2
0^+	1.176	1.2	—	0.3	nn 624↓ 624↓ 44 nn 613↑ 613↑ 1	nn 734↑ 734↑ 38 nn 631↓ 631↓ 1	nn 613↑ 624↓ 7 pp 642↑ 642↑ 1

TABLE 18. Two-quasiparticle and single-phonon states of ^{248}Cm.

Two-quasiparticle proton states: Configuration		K^π	Energy, MeV: Experiment	Energy, MeV: Calculation	Two-quasiparticle neutron states: Configuration		K^π	Energy, MeV: Experiment	Energy, MeV: Calculation
F 523↓	$F+1$ 521↑	4^+ 1^+	—	1.3	F 734↑	$F+1$ 613↑	1^-c 8^-	—	1.2
F 523↓	$F+2$ 633↑	6^- 1^-c	—	1.4	$F-1$ 624↓	$F+1$ 613↑	7^+ 0^+c	—	1.2
$F-1$ 642↑	$F+1$ 521↑	1^-c 4^-	—	1.6	F 734↑	$F+2$ 620↑	4^- 5^-	—	1.4
$F-1$ 642↑	$F+2$ 633↑	1^+ 6^+	—	1.6	$F-1$ 624↓	$F+2$ 620↑	4^+ 3^+	—	1.4
$F+1$ 521↑	$F+2$ 633↑	2^-c 5^-	—	1.9	F 734↑	$F+3$ 725↑	1^+ 10^+	—	1.6
$F-1$ 642↑	F 523↓	5^- 0^-c	—	2.0	$F-1$ 624↓	F 734↑	8^- 1^-c	—	1.6
$F-2$ 530↑	$F+1$ 521↑	1^+ 2^+c	—	2.1	$F-1$ 624↓	$F+3$ 725↑	9^- 2^-c	—	1.6
					F 734↑	$F+4$ 622↓	6^- 3^-c	—	1.6

Single-phonon states

K^π	Energy, MeV: Experiment	Energy, MeV: Calculation	$B(E\lambda)_{s.p.u.}$: Experiment	$B(E\lambda)_{s.p.u.}$: Calculation	Structure, %		
2^+	—	0.90	—	2.6	*nn* 624↓ 622↓ 39 *pp* 633↑ 402↓ 2	*nn* 622↓ 620↑ 19 *nn* 613↑ 611↑ 2	*nn* 622↑ 620↑ 15 *nn* 624↓ 611↑ 2
0^+	—	1.00	—	0.2	*nn* 734↑ 734↑ 25 *nn* 615↓ 615↓ 9	*pp* 521↑ 521↑ 15 *pp* 642↑ 642↑ 9	*pp* 523↓ 523↓ 11 *pp* 633↑ 633↑ 8
2^-	—	1.00	—	10.4	*pp* 633↑ 521↑ 29 *nn* 725↑ 613↑ 7	*nn* 725↑ 624↓ 21 *nn* 734↑ 633↓ 2	*nn* 734↑ 622↑ 14 *pp* 514↓ 651↑ 2
0^-	—	1.10	—	14.2	*nn* 615↓ 734↑ 32 *nn* 624↓ 743↑ 4	*pp* 402↓ 621↑ 8 *nn* 400↑ 501↓ 3	*pp* 642↑ 523↓ 6 *pp* 642↑ 512↑ 3
1^-	—	1.10	—	5.1	*nn* 734↑ 624↓ 38 *pp* 633↑ 523↓ 1	*nn* 734↑ 613↑ 38 *pp* 521↑ 400↑ *n*	*pp* 642↑ 521↑ 12 *nn* 725↑ 615↓ 1
3^-	—	1.54	—	0.5	*nn* 734↑ 622↓ 93	*pp* 633↑ 530↑ 1	*nn* 725↑ 622↑ 1

The energies of the octupole states with $K^\pi=0^-, 2^-$ of ^{240}Pu are well reproduced in the calculation (Table 15). It can be seen that the first $K^\pi=2^+$ state is a two-quasiparticle state and the second is a collective state. The small value of $\varkappa^{(2)}$ can cause the first state to become collective, and the second a two-quasiparticle state.

It has been established experimentally that the β^- decay of the ^{240}Np ground state and electron capture in ^{240}Am proceed entirely to the 5^- and 3^+ two-quasiparticle states at 1308 keV and 1031 keV, respectively, which are well described theoretically (see Table 15).

In the (p, t) reaction,[31] two close 0^+ levels have been observed in ^{240}Pu at 862 and 1091 keV, and it has been concluded from the analysis of the excitation cross sections that these levels differ from pure β vibrations and from simple pairing vibrations. In Ref. 81, Schmorak *et al.* analyze data on the β^- decay of ^{240m}Np and show that the level 1410 keV with $K^\pi=0^+$ is a two-phonon octupole state.

The results of the calculations of the 0^+ states given in Table 2 show that the first two 0^+ states have a complicated structure: In the first of them, the main contribution is made by a quadrupole phonon, and in the second, by the two-phonon component (301, 301), which corresponds to the conclusion drawn in Ref. 81 about the structure of the 0^+ state at 1410 keV.

7. ISOTOPES OF CURIUM AND TRANSCURIUM ELEMENTS

We now analyze the experimental data and calculations for nonrotational states of even–even isotopes of curium, californium, fermium, the element with $Z=102$, and kurchatovium. So far, these nuclei have not been studied experimentally so much as the lighter actinides. The experimentally data obtained from α and β decay and electron capture have been systematized in Refs. 1–3 and 28.

The nucleus ^{244}Cm was studied by means of the β^- decay of ^{244}Am and electron capture in ^{244}Bk, which have a decay energy of about 1.5 and 2.3 MeV, respectively, and also in the α decay of ^{248}Cf. Besides the rotational band of the ground state, there is good identification for only the level 1042 keV with $K^\pi=6^+$, to which 100% of the β^- decay from the ground state of ^{244}Am, which has the structure $p523\downarrow n624\downarrow$, takes place. In our calculations (Table 16) it corresponds to the two quasi-particle state 1.0 MeV, $nn622\uparrow 624\downarrow$, which agrees well with the experiment.

The nucleus ^{244}Cm has also been studied in Ref. 30 by means of Coulomb excitation in the (α, α') reaction, although data on the positions of the bases of the rotational bands have not been obtained.

The ^{246}Cm nucleus is the best studied isotope of curium. The excitation spectrum of ^{246}Cm was obtained

TABLE 19. Two-quasiparticle and single-phonon states of ^{248}Cf.

Two-quasiparticle proton states: Configuration		K^π	Energy, MeV: Experiment	Energy, MeV: Calculation	Two-quasiparticle neutron states: Configuration		K^π	Energy, MeV: Experiment	Energy, MeV: Calculation
F 521↑	$F+1$ 633↑	2^-c 5^-	—	0.9	F 624↓	$F+1$ 734↑	8^- 1^-c	—	0.8
F 521↑	$F+2$ 514↓	5^+ 2^+c	—	1.7	F 624↓	$F+2$ 613↑	7^+ 0^+c	—	1.3
$F-1$ 523↓	$F+1$ 633↑	6^- 1^-c	—	1.8	$F-1$ 622↑	$F+1$ 734↑	2^-c 7^-	—	1.5
$F+1$ 633↑	$F+2$ 514↓	7^- 0^-c	—	1.8	$F+1$ 734↑	$F+2$ 613↑	1^-c 8^-	—	1.5
$F-1$ 523↓	F 521↑	4^+ 1^+	—	1.8	$F-2$ 743↑	$F+1$ 734↑	1^+ 8^+	—	1.5
$F-2$ 642↑	$F+1$ 633↑	1^+ 6^+	—	2.0	$F-3$ 631↓	$F+1$ 734↑	5^- 4^-	—	1.6
$F-2$ 642↑	F 521↑	1^-c 4^-	—	2.0	$F-1$ 622↑	F 624↓	6^+ 1^+	—	1.6

Single-phonon states

K^π	Energy, MeV: Experiment	Energy, MeV: Calculation	$B(E\lambda)_{s.p.u.}$: Experiment	$B(E\lambda)_{s.p.u.}$: Calculation	Structure, %		
1^-	—	0.7	—	0.07	*nn* 734↑ 624↓ 100	— — —	— — —
2^-	0.593	0.7	—	7.3	*pp* 633↑ 521↑ 65 *nn* 734↑ 633↓ 2	*nn* 734↑ 622↑ 16 *pp* 514↓ 651↑ 1	*nn* 725↑ 624↓ 6 *nn* 631↓ 752↓ 1
0^+	—	1.00	—	0.4	*nn* 624↓ 624↓ 52 *pp* 514↓ 514↓ 2	*nn* 734↑ 734↑ 36 *pp* 633↑ 633↑ 1	*nn* 613↑ 624↓ 5 *nn* 615↓ 615↓ 1
0^-	—	1.10	—	12.4	*nn* 624↓ 743↑ 38 *nn* 400↑ 501↓ 3	*pp* 633↑ 514↓ 12 *pp* 402↓ 521↑ 3	*nn* 615↓ 734↑ 5 *pp* 642↑ 512↑ 3
2^+	—	1.20	—	1.8	*nn* 624↓ 622↓ 47 *nn* 622↓ 620↑ 3	*nn* 622↑ 620↑ 24 *nn* 734↑ 752↑ 2	*pp* 521↑ 521↓ 5 *nn* 725↑ 743↑ 2
2^-	1.477	1.35	—	0.6	*nn* 734↑ 622↑ 62 *nn* 734↑ 633↓ 1	*pp* 633↑ 521↑ 30 — — —	*nn* 725↑ 624↓ 4 — — —
3^-	—	1.83	—	1.0	*nn* 734↑ 622↓ 70 *nn* 716↑ 624↓ 2	*pp* 624↑ 521↑ 16 *pp* 633↑ 530↑ 1	*nn* 725↑ 622↑ 4 *nn* 615↓ 501↑ 1

TABLE 20. Two-quasiparticle and single-phonon states of ^{250}Cf.

Two-quasiparticle proton states					Two-quasiparticle neutron states				
Configuration		K^π	Energy, MeV: Experiment	Energy, MeV: Calculation	Configuration		K^π	Energy, MeV: Experiment	Energy, MeV: Calculation
F 633↑	$F+1$ 521↑	2^-c 5^-	—	1.0	F 734↑	$F+1$ 613↑	1^-c 8^-	—	1.2
F 633↑	$F+2$ 514↓	7^- 0^-c	—	1.8	$F-1$ 624↓	$F+1$ 613↑	7^+ 0^+c	—	1.2
$F+1$ 521↑	$F+2$ 514↓	5^+ 2^+c	—	1.9	F 734↑	$F+2$ 620↑	4^- 5^-	—	1.4
$F-1$ 642↑	$F+1$ 521↑	1^-c 4^-	—	2.1	$F-1$ 624↓	$F+2$ 620↑	4^+ 3^+	—	1.4
$F-2$ 400↑	$F+1$ 521↑	1^-c 2^-c	—	2.1	F 734↑	$F+3$ 725↑	1^+ 10^+	—	1.6
$F-3$ 523↓	$F+1$ 521↑	4^+ 1^+	—	2.1	$F-1$ 624↓	F 734↑	8^- 1^-c	—	1.6
$F-1$ 642↑	F 633↑	1^+ 6^+	—	2.2	$F-1$ 624↓	$F+3$ 725↑	9^- 2^-c	—	1.6
$F-2$ 400↑	F 633↑	3^+ 4^+	—	2.2	F 734↑	$F+4$ 622↓	6^- 3^-c	—	1.6

Single-phonon states

K^π	Energy, MeV: Experiment	Energy, MeV: Calculation	$B(E\lambda)_{s.p.u.}$: Experiment	$B(E\lambda)_{s.p.u.}$: Calculation	Structure, %		
0^+	—	0.9	—	5.3	nn734↑ 734↑ 24 nn725↑ 725↑ 4	nn613↑ 624↑ 19 pp514↓ 514↓ 4	nn613↑ 613↑ 13 nn615↓ 615↓ 4
2^+	1.032	0.9	—	5.2	nn624↓ 622↓ 38 pp521↑ 521↓ 4	nn622↑ 620↑ 16 nn613↑ 611↑ 2	nn622↓ 620↑ 16 pp523↓ 521↓ 2
2^-	0.871	1.0	—	6.8	pp633↑ 521↑ 38 nn734↑ 622↑ 5	nn725↑ 624↓ 20 pp514↓ 651↑ 2	nn725↑ 613↑ 10 nn613↑ 761↑ 2
1^-	1.176	1.0	—	11.9	nn734↑ 624↓ 28 nn620↑ 770↑ 2	nn734↑ 613↑ 24 pp521↑ 660↑ 2	pp642↑ 521↑ 6 nn752↑ 622↓ 2
0^-	—	1.1	—	13.4	pp633↑ 514↓ 6 nn600↑ 770↑ 4	nn611↓ 501↓ 5 nn615↓ 734↑ 4	nn602↓ 501↑ 5 nn606↑ 716↑ 4

in the β^- decay of two isomers of ^{246}Am: $T_{1/2}=25$ and 39 min, which have decay energy 2.3 MeV, and also in electron capture processes in ^{246}Bk and the α decay of ^{250}Cf. In Ref. 31 [(p, t) reaction] data are given on a level at 1176 keV with $K^\pi=0^+$. The energies of the first quadrupole and octupole states with $K^\pi=0^-, 1^-, 2^-$ are reproduced well in the calculations (Table 17). In the (α, α') reaction,[30] a level was observed at 1124 keV with $K^\pi=2^+$, which confirms the previously known energy of this state; the $B(E2, 0_g \to I=2, K=2)_{exp}$ value agrees with the results of the calculation.

In the β^- decay of the isomer ^{246}Am, $T_{1/2}=39$ min, one can see clearly an 8^- level that does not belong to rotational bands based on octupole states. According to the calculations, the two-quasiparticle state $nn624\downarrow 734\uparrow$ $K^\pi=8^-$ has energy 0.8 MeV and can be populated by a β transition from the state $p523\downarrow + n734\uparrow$. When there is β decay from the states $p523\downarrow \pm 734\uparrow$ one should observe several of the two-quasiparticle states given in Table 17.

In the excitation spectrum of ^{248}Cm only the rotational band of the ground state has been established.[3] Some excited levels of positive and negative parity were established in Ref. 30, but the positions of the bases of the rotational bands were not determined. There is an α transition from ^{252}Cf to a collective state with energy 0.68 MeV, but the quantum numbers of this level were not established. Calculations of the nonrotational states of ^{248}Cm are given in Table 18.

In Ref. 82, two excited states of ^{248}Cf with energies 593 and 1477 keV and with $K^\pi=2^-$ were observed. In our calculations for ^{248}Cf (Table 19) the first two states with $K^\pi=2^-$ have energies 0.7 and 1.4 MeV.

In ^{250}Cf, β^- decay of ^{250}Bk established the first quadrupole state with $K^\pi=2^+$, $E=1032$ keV, to which 89% of the decay takes place. In Refs. 37 and 83 in ^{250}Cf, octupole states with $K^\pi=1^-$, $E=1175.5$ keV and with $K^\pi=2^-$, $E=871.4$ keV were observed. As can be seen from Table 20, the energies of these states are well reproduced by the calculations.

It is impossible to investigate the excited states of ^{252}Cf by means of β^- decay since the nucleus ^{252}Bk is not observed experimentally. The excitation spectrum of ^{252}Cf was investigated in Ref. 84, in which levels with $K^\pi=2^+$, $E=805$ keV and with $K^\pi=2^-$, $E=831$ keV were established, and also a two-quasiparticle state with $K^\pi=3^+$ $nn613\uparrow 620\uparrow$. It can be seen from Table 21 that these states can be described perfectly satisfactorily.

The experimental data on levels of ^{254}Fm have been obtained solely from β^- decay of the isomer ^{254}Es ($T_{1/2}=39.6$ h). Besides levels of the rotational band of the ground state one can clearly see (77% of the decay) the first two levels of the band based on the quadrupole

TABLE 21. Two-quasiparticle and single-phonon states of ^{252}Cf.

Two-quasiparticle proton states					Two-quasiparticle neutron states				
Configuration		K^π	Energy, MeV: Experiment	Energy, MeV: Calculation	Configuration		K^π	Energy, MeV: Experiment	Energy, MeV: Calculation
F 633↑	$F+1$ 521↑	2^-c 5^-	—	1.0	F 613↑	$F+1$ 620↑	3^+ 4^+	0.97	1.1
F 633↑	$F+2$ 514↓	7^- 0^-c	—	1.8	F 613↑	$F+2$ 725↑	2^-c 9^-	—	1.3
$F+1$ 521↑	$F+2$ 514↓	5^+ 2^+c	—	1.9	F 613↑	$F+3$ 622↑	5^+ 2^+c	—	1.3
$F-1$ 642↑	$F+1$ 521↑	1^-c 4^-	—	2.1	$F+1$ 620↑	$F+2$ 725↑	5^- 6^-	—	1.4
$F-2$ 400↑	$F+1$ 521↑	1^-c 2^-c	—	2.1	$F+1$ 620↑	$F+3$ 622↑	2^+c 1^+	—	1.5
$F-3$ 523↓	$F+1$ 521↑	4^+ 1^+	—	2.1	$F-1$ 734↑	$F+1$ 620↑	4^- 5^-	—	1.6
$F-1$ 642↑	F 633↑	1^+ 6^+	—	2.2	$F-1$ 734↑	F 613↑	1^-c 8^-	—	1.6
$F-2$ 400↑	F 633↑	3^+ 4^+	—	2.2	$F+2$ 725↑	$F+3$ 622↑	7^- 4^-	—	1.7

Single-phonon states

K^π	Energy, MeV: Experiment	Energy, MeV: Calculation	$B(E\lambda)_{s.p u.}$: Experiment	$B(E\lambda)_{s.p u.}$: Calculation	Structure, %		
2^+	0.805	0.7	—	5.7	nn622↓ 620↑ 43 nn613↑ 611↑ 4	nn624↓ 622↓ 22 pp521↑ 521↓ 3	nn622↑ 620↑ 8 pp523↓ 521↓ 1
2^-	0.831	0.9	—	8.8	nn725↑ 613↑ 33 pp514↓ 651↑ 1	pp633↑ 521↑ 31 nn611↑ 770↑ 1	nn725↑ 624↓ 13 nn734↑ 622↑ 1
0^-	—	1.0	—	15.8	nn611↓ 501↓ 5 nn602↓ 501↑ 5	nn620↑ 761↑ 5 nn600↑ 700↑ 4	pp633↑ 514↓ 5 nn615↓ 734↑ 4
1^-	—	1.0	—	18.2	nn734↑ 613↑ 15 nn725↑ 615↓ 4	pp642↑ 521↑ 8 pp521↑ 660↑ 3	nn734↑ 624↑ 5 nn620↑ 761↓ 3
0^+	—	1.1	—	6.1	nn613↑ 624↓ 16 nn613↑ 613↑ 8	nn620↑ 620↑ 14 nn734↑ 734↑ 8	nn615↓ 615↓ 10 pp514↓ 514↓ 6

TABLE 22. Two-quasiparticle and single-phonon states of ^{254}Fm.

Two-quasiparticle proton states					Two-quasiparticle neutron states				
Configuration		K^π	Energy, MeV		Configuration		K^π	Energy, MeV	
			Experiment	Calculation				Experiment	Calculation
F 521↑	$F+1$ 514↓	5^+ 2^+c	—	1.3	F 613↑	$F+1$ 620↑	3^+ 4^+	— —	1.1
$F-1$ 633↑	$F+1$ 514↓	7^- 0^-c	—	1.3	F 613↑	$F+2$ 725↑	2^-c 9^-	—	1.3
F 521↑	$F+2$ 624↑	3^-c 6^-	—	1.7	F 613↑	$F+3$ 622↓	5^+ 2^+c	—	1.3
$F-1$ 633↑	$F+2$ 624↑	1^+ 8^+	—	1.8	$F+1$ 620↑	$F+2$ 725↑	5^- 6^-	—	1.4
F 521↑	$F+3$ 521↑	2^+c 1^+	—	1.9	$F+1$ 620↑	$F+3$ 622↓	2^+c 1^+	—	1.5
$F-1$ 633↑	$F+3$ 521↓	4^- 3^-c	—	2.0	$F-1$ 734↑	$F+1$ 620↑	4^- 5^-	—	1.6
$F-1$ 633↑	F 521↓	2^-c 5^-	—	2.0	$F-1$ 734↑	F 613↑	1^-c 8^-	—	1.6
$F+1$ 514↓	$F+2$ 624↑	8^- 1^-c	—	2.1	$F+2$ 725↑	$F+3$ 622↑	7^- 4^-	—	1.7

Single-phonon states

K^π	Energy, MeV		$B(E\lambda)_{s.p.u.}$		Structure, %		
	Experiment	Calculation	Experiment	Calculation			
2^+	0.693	0.8	—	4.6	nn622↓ 620↑ 45 pp521↑ 521↓ 6	nn624↓ 622↓ 22 nn613↑ 611↑ 4	nn622↑ 620↑ 7 pp523↓ 521↓ 1
2^-	—	1.0	—	4.9	nn725↑ 613↑ 45 pp514↓ 651↑ 1	nn725↑ 624↓ 17 nn611↑ 770↑ 1	pp633↑ 521↑ 12 nn734↑ 622↑ 1
0^-	—	1.1	—	12.7	pp633↑ 514↓ 11 nn602↓ 501↑ 4	nn611↓ 501↓ 5 nn615↓ 734↑ 4	nn620↑ 761↓ 5 nn600↑ 770↑ 4
0^+	—	1.1	—	3.1	pp514↓ 514↓ 25 nn613↑ 624↓ 9	pp633↑ 633↑ 12 nn620↑ 620↑ 8	pp521↑ 521↑ 11 nn615↓ 615↓ 5
1^-	—	1.2	—	15.0	nn734↑ 613↑ 20 nn725↑ 615↓ 4	nn734↑ 624↓ 6 nn620↑ 761↓ 3	pp633↑ 512↑ 5 nn622↓ 761↓ 3

state with $K^\pi = 2^+$, $E = 693$ keV. In calculations of the nonrotational states for ^{254}Fm (Table 22), the energy of this state is reproduced satisfactorily.

At present, there are no experimental data on excited states of the heavier even–even fermium isotopes or the even–even isotopes of nuclei with $Z = 102$. An element with $Z = 104$ has been discovered by Flerov's group[85] and called kurchatovium. In Tables 23–25, we give the results of calculations of single-phonon and two-quasiparticles states of ^{256}Fm, ^{254}102, and ^{260}Ku.

The insufficient experimental data on states in the even–even isotopes of the heavy actinides (curium and transcurium elements) do not allow us to make a more detailed comparison of the results of our calculations with experiments, and also restricts the possibility of an unambiguous choice of the parameters of the model. We hope that the present paper will be helpful for the further comprehensive study of the nuclei of heavy actinides.

CONCLUSIONS

As a result of our investigations, we can conclude that the superfluid model of the nucleus gives a good description of the properties of the low-lying nonrotational states of even–even nuclei in the region of the actinides.

The structure of the lowest excited states is comparatively simple: In the majority of cases, they are two-quasiparticle or single-phonon excitations. Many of the predictions of the earlier theory of two-quasiparticle states were subsequently confirmed experimentally. The further discovery of such states will make it possible to determine the parameters of the average field and the interaction constant more accurately.

However, in some cases (this applies especially to the nuclei of the transition region) the structure of the states is more complicated. In the calculations, it is necessary to take into account the effects of anharmonicity. The most complicated structure is that of the 0^+ states, the lowest of which may sometimes contain a large admixture of a two-phonon component. It should be noted that when allowance is made for anharmonicity the constants of the multipole–multipole interaction for which the calculated energies agree with the experimental energies approach constants for each zone.

The investigation of states with high excitation energy (≥ 2 MeV) shows that they have an even more complicated structure. Besides the effects of anharmonicity, one must take into account interaction between the two-quasiparticle and the vibrational degrees of freedom, and also the interaction between the internal motion and the rotational motion. At the present time, these investigations are only beginning.

The theoretical description of nuclei in the region of

TABLE 23. Two-quasiparticle and single-phonon states of ^{256}Fm.

Two-quasiparticle proton states					Two-quasiparticle neutron states				
Configuration		K^π	Energy, MeV		Configuration		K^π	Energy, MeV	
			Experiment	Calculation				Experiment	Calculation
F 521↑	$F+1$ 514↓	5^+ 2^+c	—	1.3	F 620↑	$F+1$ 725↑	5^- 6^-	—	1.2
$F-1$ 633↑	$F+1$ 514↓	7^- 0^-c	—	1.3	F 620↑	$F+2$ 622↓	2^+c 1^+	—	1.2
F 521↑	$F+2$ 624↑	3^-c 6^-	—	1.7	$F-1$ 613↑	$F+1$ 725↑	2^-c 9^-	—	1.3
$F-1$ 633↑	$F+2$ 624↑	1^+ 8^+	—	1.8	$F-1$ 613↑	F 620↑	3^+ 4^+	—	1.3
F 521↑	$F+3$ 521↓	2^+c 1^+	—	1.9	$F-1$ 613↑	$F+2$ 622↓	5^+ 2^+c	—	1.3
$F-1$ 633↑	$F+3$ 521↓	4^- 3^-c	—	2.0	$F+1$ 725↑	$F+2$ 622↓	7^- 4^-	—	1.3
$F-1$ 633↑	F 521↑	2^-c 5^-	—	2.0	F 620↑	$F+3$ 615↓	5^+ 4^+	—	1.7

Single-phonon states

K^π	Energy, MeV		$B(E\lambda)_{s.p.u.}$		Structure, %		
	Experiment	Calculation	Experiment	Calculation			
2^+	—	0.7	—	5.3	nn622↓ 620↑ 57 pp521↑ 521↓ 6	nn624↓ 622↓ 12 nn622↑ 620↑ 3	nn613↑ 611↑ 6 nn615↓ 613↓ 1
0^-	—	0.8	—	17.2	nn620↑ 761↓ 9 nn611↓ 501↓ 5	pp633↑ 613↑ 7 nn602↓ 501↑ 4	nn622↓ 752↓ 5 nn600↑ 770↑ 4
0^+	—	0.9	—	5.0	pp514↓ 514↓ 21 pp633↑ 633↑ 10	nn615↓ 615↓ 16 pp521↑ 521↑ 8	nn620↑ 620↑ 14 nn613↑ 624↓ 3
2^-	—	1.0	—	6.1	nn725↓ 613↑ 47 nn716↑ 615↓ 2	pp633↑ 521↑ 12 pp514↓ 651↑ 2	nn725↑ 624↓ 10 nn622↓ 761↓ 1
1^-	—	1.1	—	15.9	nn725↑ 615↓ 13 nn734↑ 613↑ 6	nn622↓ 761↓ 8 pp633↑ 512↑ 5	nn620↑ 761↓ 6 nn752↓ 620↑ 5

TABLE 24. Two-quasiparticle and single-phonon states of $^{254}102$.

Two-quasiparticle proton states					Two-quasiparticle neutron states				
Configuration		K^π	Energy, MeV Experiment	Energy, MeV Calculation	Configuration		K^π	Energy, MeV Experiment	Energy, MeV Calculation
F 514↓	$F+1$ 624↑	8^- 1^-c	—	1.1	F 734↑	$F+1$ 613↑	1^-c 8^-	—	1.2
F 514↓	$F+2$ 521↓	3^+ 4^+	—	1.3	$F-1$ 624↓	$F+1$ 613↑	7^+ 0^+c	—	1.2
$F+1$ 624↓	$F+2$ 521↓	5^- 4^-	—	1.7	F 734↑	$F+2$ 620↑	4^- 5^-	—	1.4
F 514↓	$F+3$ 512↑	6^+ 1^+	—	1.8	$F-1$ 624↓	$F+2$ 620↑	4^+ 3^+	—	1.4
$F-1$ 521↑	$F+1$ 624↑	3^-c 6^-	—	1.9	F 734↑	$F+3$ 725↑	1^+ 10^+	—	1.6
$F-2$ 633↑	$F+1$ 624↑	1^+ 8^+	—	2.0	$F-1$ 624↓	F 734↑	8^- 1^-c	—	1.6
$F-1$ 521↑	$F+2$ 521↓	2^+c 1^+	—	2.0	$F-1$ 624↓	$F+3$ 725↑	9^- 2^-c	—	1.6

Single-phonon states

K^π	Energy, MeV Experiment	Energy, MeV Calculation	$B(E\lambda)_{s.p.u.}$ Experiment	$B(E\lambda)_{s.p.u.}$ Calculation	Structure, %		
1^-	—	0.9	—	15.5	nn734↑ 624↓ 25 pp624↑ 514↓ 3	nn734↑ 613↑ 21 nn620↑ 770↑ 3	pp633↑ 512↑ 4 nn752↑ 622↓ 2
0^+	—	1.0	—	2.2	nn734↑ 734↑ 29 pp514↓ 514↓ 7	nn613↑ 613↑ 16 nn725↑ 725↑ 4	nn613↑ 624↓ 15 pp521↓ 521↓ 3
2^+	—	1.1	—	3.3	nn624↓ 622↓ 41 pp521↑ 521↓ 8	nn622↓ 620↑ 16 nn613↑ 611↑ 2	nn622↑ 620↑ 16 nn725↑ 743↑ 1
0^-	—	1.3	—	11.0	nn611↓ 501↓ 5 nn602↓ 501↑ 5	pp633↑ 514↓ 5 nn600↑ 770↑ 4	nn615↓ 734↑ 5 nn624↓ 743↑ 4
2^-	—	1.3	—	4.3	nn725↑ 624↓ 38 nn734↑ 622↑ 8	nn725↑ 613↑ 18 pp633↑ 521↑ 2	pp624↑ 512↑ 9 nn613↑ 761↑ 2

TABLE 25. Two-quasiparticle and single-phonon states of ^{260}Ku.

Two-quasiparticle proton states					Two-quasiparticle neutron states				
Configuration		K^π	Energy, MeV Experiment	Energy, MeV Calculation	Configuration		K^π	Energy, Mev Experiment	Energy, Mev Calculation
F 624↑	$F+1$ 521↓	5^- 4^-	—	1.1	F 620↑	$F+1$ 725↑	5^- 6^-	—	1.2
$F-1$ 514↓	$F+1$ 521↓	3^+ 4^+	—	1.5	F 620↑	$F+2$ 622↓	2^+c 1^+	—	1.2
F 624↑	$F+2$ 512↑	2^-c 7^-	—	1.6	$F-1$ 613↑	$F+1$ 725↑	2^-c 9^-	—	1.3
$F-1$ 514↓	F 624↑	8^- 1^-c	—	1.6	$F-1$ 613↑	F 620↑	3^+ 4^+	—	1.3
$F+1$ 521↓	$F+2$ 512↑	3^+ 2^+c	—	1.7	$F-1$ 613↑	$F+2$ 622↓	5^+ 2^+c	—	1.3
F 624↑	$F+3$ 615↑	1^+ 10^+	—	2.3	$F+1$ 725↑	$F+2$ 622↓	7^- 4^-	—	1.3
$F-2$ 521↑	$F+1$ 521↓	1^+ 2^+c	—	2.3	F 620↑	$F+3$ 615↓	5^+ 4^+	—	1.7

Single-phonon states

K^π	Energy, MeV Experiment	Energy, MeV Calculation	$B(E\lambda)_{s.p.u.}$ Experiment	$B(E\lambda)_{s.p.u.}$ Calculation	Structure, %		
2^+	—	0.8	—	3.2	nn622↓ 620↑ 64 nn622↑ 620↑ 3	nn624↓ 622↓ 12 pp521↑ 521↓ 3	nn613↑ 611↑ 6 nn615↓ 613↓ 1
2^-	—	0.9	—	7.3	nn725↑ 613↑ 42 nn716↑ 615↓ 2	pp624↑ 512↑ 17 nn611↑ 770↑ 1	nn725↑ 624↓ 10 nn622↓ 761↓ 1
0^+	—	0.9	—	6.5	nn615↓ 615↓ 23 pp514↓ 514↓ 5	nn620↑ 620↑ 18 nn613↑ 624↓ 5	pp521↓ 521↓ 14 nn725↑ 725↑ 4
0^-	—	1.00	—	13.2	nn620↑ 761↓ 10 nn602↓ 501↑ 5	nn622↓ 752↓ 6 nn600↑ 770↑ 4	nn611↓ 501↑ 5 pp400↑ 510↑ 4
1^-	—	1.1	—	16.5	nn725↑ 615↓ 13 nn734↑ 613↑ 6	nn622↓ 761↓ 8 nn752↓ 620↑ 5	nn620↑ 761↓ 6 pp633↑ 512↑ 5

the actinides encounters additional difficulties associated with the fact that there is not adequate experimental information about these nuclei. However, in recent years interesting results have been obtained about the properties of nuclei in this region from the study of nuclear reactions. The use of different reactions makes it possible to clarify the finer details of the nuclear structure. It is to be hoped that a comprehensive theoretical and experimental investigation of the nuclei in the actinide region will establish the basic quantum numbers of the nuclear levels at intermediate and high excitation energies.

We should like to thank our collaborators in the Department of Nuclear Theory in the Laboratory of Theoretical Physics at Dubna for helpful comments, and also G. Kyrchev and V.O. Nesterenko for assisting in the work and helpful discussions.

[1]B. S. Dzhelepov, L.K. Peker, and V.O. Sergeev, Skhemy Raspada Radioaktivnykh Yader s $A \geq 100$ (Decay Schemes of Radioactive Nuclei with $A \geq 100$), Izd-vo Akad Nauk SSSR (1963).
[2]C.M. Lederer, J.M. Hollander, and I. Perlman, Table of Isotopes, Sixth Edition, Wiley, New York (1967).
[3]Nuclear Level Schemes $A=45$ through $A=257$ from Nuclear Data Sheets, Academic Press, Inc., New York and London (1973); Y.A. Ellis and M.R. Schmorak, Nucl. Data Sheets 8, No. 4 (1972).
[4]N.A. Voinova and B.S. Dzhelepov, Izobarnye Yadra s Massovym Chislom $A=182$ (Isobaric Nuclei with Mass Number $A=182$), Nauka, Moscow (1968).
[5]V.P. Grigor'ev and V.G. Solov'ev, Struktura Chetnykh Deformirovannykh Yader (Structure of Even Deformed Nuclei), Nauka, Moscow (1974).
[6]A. Bohr and B.R. Mottelson, Nuclear Structure, Vol. 1, New York (1969).
[7]G.E. Brown, Unified Theory of Nuclear Models and Forces, 2nd ed., North Holland (1967); A.B. Migdal, Teoriya Konechnykh Fermi-Sistem i Svoǐstva Atomnykh Yader, Nauka, Moscow (1965) [Translation: Theory of Finite Fermi Systems, Interscience, New York (1967)].
[8]V.G. Solov'ev, Teoriya Slozhnykh Yader (Theory of Complex Nuclei), Nauka, Moscow (1971).
[9]C.J. Gallagher and V.G. Soloviev, Mat. Fys. Skr. Dan. Vid. Selsk. 2, 2 (1962); V.G. Soloviev, Atomic Energy Rev. 3, No. 2, 117 (1965).
[10]V.G. Solov'ev, Zh. Éksp. Teor. Fiz. 40, 654 (1961) [Sov. Phys. JETP 13, 456 (1961)]; T. Veresh, V.G. Solov'ev, and T. Sikloš, Izv. Akad. Nauk SSSR, Ser. Fiz. 26, 1045 (1962); V.G. Soloviev and P. Vogel, Phys. Lett. 6, 126 (1963); V.G. Soloviev and T. Sikloš, Nucl. Phys. 59, 145 (1964); Liu Yuan, V.G. Solov'ev, and A.A. Korneǐchuk, Zh. Éksp. Teor. Fiz. 47, 252 (1964) [Sov. Phys. JETP 20, 169 (1965)]; V.G. Solov'ev, P. Vogel, and A.A. Korneǐchuk, Izv. Akad. Nauk SSSR, Ser. Fiz. 28, 1599 (1964); L.A. Malov, V.G. Soloviev, and P. Vogel, Phys. Lett. 22, 441 (1966).
[11]A.L. Komov, L.A. Malov, and V.G. Solov'ev, Soobshchenie (Communication), JINR R4-5126 (1970); Izv. Akad. Nauk SSSR, Ser. Fiz. 35, 1550 (1971); S.P. Ivanova, A.L. Malov, and V.G. Solov'ev, Preprint JINR R4-8459 (1974); Izv. Akad. Nauk SSSR, Ser. Fiz. 39, 1286 (1975).

[12]L. A. Malov and V. G. Solov'ev, Yad. Fiz. 5, 566 (1967) [Sov. J. Nucl. Phys. 5, 403 (1967)]; A. L. Komov, L. A. Malov, and V. G. Solov'ev, Soobshchenie (Communication), JINR R4-5693 (1971); S. P. Ivanova, A. L. Komov, L. A. Malov, and V. G. Solov'ev, Izv. Akad. Nauk SSSR, Ser. Fiz. 37, 911 (1973); S. P. Ivanova, A. L. Komov, L. A. Malov, and V. G. Solov'ev, Preprint JINR R4-8582 (1975); Izv. Akad. Nauk SSSR, Ser. Fiz. 39, 1612 (1975).
[13]F. A. Gareev, S. P. Ivanova, L. A. Malov, and V. G. Soloviev, Nucl. Phys. A 171, 134 (1971).
[14]R. V. Jolos, V. G. Soloviev, and K. M. Zheleznova, Phys. Lett. B 25, 393 (1967); R. V. Jolos, U. M. Finer, V. G. Soloviev, and K. M. Zheleznova, Phys. Lett. B 27, 614 (1968).
[15]G. Kyrchev, V. G. Solov'ev, and Ch. Stoyanov, Izv. Akad. Nauk SSSR, Ser. Fiz. (1975); Preprint JINR R4-8611 (1975).
[16]S. P. Ivanova, A. L. Komov, G. Kyrchev, V. G. Solov'ev, and Ch. Stoyanov, Tezisy XXVI Soveshchaniya po Yadernoĭ Spektroskopii i Strukture Yadra (Proc. 26th Conference on Nuclear Spectroscopy and Nuclear Structure), Baku (1976).
[17]S. P. Ivanova, A. L. Komov, G. Kyrchev, V. G. Soloviev, and Ch. Stojanov, Preprint JINR E4-9010 (1975).
[18]V. G. Soloviev, Nucl. Phys. 69, 1 (1965).
[19]A. Bohr, Nuclear Structure, Dubna Symposium 1968, IAEA, Vienna (1968), p. 179; J. O. Rasmussen, Nuclear Structure, Dubna Symposium 1968, IAEA, Vienna (1968), p. 169; R. A. Sorensen, Nuclear Structure, Dubna Symposium 1968, IAEA, Vienna (1969), p. 27; S. T. Belyaev, Nuclear Structure, Dubna Symposium 1968, IAEA, Vienna (1968), p. 155; N. I. Pyatov, Arkiv. Fys. 36, 667 (1967).
[20]B. N. Kalinkin, Ya. Grabovski, and F. A. Gareev, Acta. Phys. Pol. 30, 999 (1966); F. A. Gareev, S. P. Ivanova, and B. N. Kalinkin, Acta Phys. Pol. 30, 461 (1966); F. A. Gareev, S. P. Ivanova, and B. N. Kalinkin, Izv. Akad. Nauk SSSR, Ser. Fiz. 33, 1690 (1968).
[21]F. A. Gareev, S. P. Ivanova, V. G. Solov'ev, and S. I. Fedotov, Fiz. Élem. Chastits At. Yadra. 4, 357 (1973) [Sov. J. Part. Nucl. 4, 148 (1973)].
[22]F. A. Gareev, S. P. Ivanova, and V. V. Pashkevich, Yad. Fiz. 11, 1200 (1970) [Sov. J. Nucl. Phys. 11, 667 (1970)]; Preprint JINR E4-4704 (1969); S. P. Ivanova, A. L. Komov, and N. Yu. Shirikova, Soobshchenie (Communication), JINR R4-8406 (1974).
[23]C. E. Bemis *et al.*, Phys. Rev. C 8, 1466 (1973).
[24]J. L. C. Ford *et al.*, Phys. Rev. Lett. 27, 1232 (1971); F. K. McGowan *et al.*, Phys. Rev. Lett. 27, 1741 (1971).
[25]V. M. Strutinskiĭ, Yad. Fiz. 3, 614 (1966) [Sov. J. Nucl. Phys. 3, 449 (1966)]; Nucl. Phys. A 95, 420 (1967).
[26]N. P. Newly, Phys. Rev. 125, 2063 (1962); N. I. Pyatov, Izv. Akad. Nauk SSSR, Ser. Fiz. 27, 1436 (1963); N. I. Pyatov and A. S. Chernyshev, Izv. Akad. Nauk SSSR, Ser. Fiz. 28, 1173 (1964).
[27]E. Arbman *et al.*, Nucl. Phys. 21, 406 (1960); M. Arnoux *et al.*, Compt. Rend. 169, 317 (1969); M. Herment *et al.*, Compt. Rend. 273, 801, 1053 (1971); W. Kurcewicz *et al.*, J. Phys. (Paris) 34, 159 (1973); J. Dalmasso *et al.*, C.R. Acad. Sci. Ser. B 278, 97 (1974); J. Dalmasso *et al.*, Compt. Rend. 273, 509, 568 (1971).
[28]V. M. Gorbachev, Yu. S. Zamyatin, and A. A. Lbov, Osnovnye Kharakteristiki Izotopov Tyazhelykh Élementov (Basic Quantum Numbers of Isotopes of Heavy Elements), Second Edition, Atomizdat, Moscow (1975).
[29]Th. W. Else and J. R. Huizenga, Nucl. Phys. A 187, 545 (1972).
[30]F. K. McGowan *et al.*, Phys. Rev. C 10, 1146 (1974).
[31]J. V. Maher *et al.*, Phys. Rev. C 5, 1380 (1972).
[32]R. F. Casten *et al.*, Phys. Lett. B 40, 333 (1972).
[33]B. B. Back *et al.*, Nucl. Phys. A 217, 116 (1973).
[34]W. R. McMurray *et al.*, Z. Phys. 253, 289 (1972).
[35]F. S. Stephens, F. Asaro, and I. Perlman, Phys. Rev. 100, 1543 (1955).
[36]T. Yamazaki, Nucl. Data A 1, 453 (1966).
[37]F. S. Stephens *et al.*, Phys. Rev. Lett. 15, 420 (1965).
[38]S. Bjørnholm *et al.*, Nucl. Phys. A 118, 261 (1968).
[39]K. Neergard and P. Vogel, Nucl. Phys. 149, 217 (1970).
[40]S. Bjørnholm *et al.*, Nucl. Phys. 42, 469 (1963).
[41]S. A. Baranov *et al.*, Zh Éksp. Teor. Fiz. 41, 1475 (1961) [Sov. Phys. JETP 14, 1053 (1962)].
[42]R. E. Bell *et al.*, Kgl. Dan. Vid. Selsk. Mat.-Fys. Medd. 32, No. 12 (1960).
[43]L. Varnell, Nucl. Phys. A 144, 429 (1970).
[44]C. M. Lederer, Thesis, Univ. California (1963); UCRL-11028 (1963).
[45]S. A. Baranov *et al.*, Yad. Fiz. 5, 241 (1967) [Sov. J. Nucl. Phys. 5, 169 (1967)].
[46]A. Bjørnholm and O. B. Nielsen, Nucl. Phys. 42, 642 (1963).
[47]A. H. Wapstra, Nucl. Phys. A 97, 641 (1967).
[48]A. H. Wapstra, Physica 37, 261 (1967).
[49]G. Ardisson and C. Ardisson, Compt. Rend. Ser. B 280, 377 (1975).
[50]P. W. De Lange *et al.*, Nuovo Cimento 14, 681 (1959).
[51]Ong Ping Hok, Physica 22, 465 (1956).
[52]P. G. Hansen *et al.*, Phys. Lett. B 24, 95 (1967).
[53]C.-F. Leang, Compt. Rend. 255, 3155 (1962).
[54]S. A. Baranov *et al.*, Yad. Fiz. 7, 727 (1968) [Sov. J. Nucl. Phys. 7, 442 (1968)].
[55]E. K. Hyde *et al.*, The Nuclear Properties of the Heavy Elements, Vol. II, Prentice-Hall, Englewood Cliffs, New Jersey (1964).
[56]S. Bjørnholm *et al.*, Phys. Rev. 130, 2000 (1963).
[57]S. Bjørnholm *et al.*, Nucl. Phys. A 118, 241 (1968).
[58]J. S. Boyno *et al.*, Nucl. Phys. A 209, 125 (1973).
[59]N. Trautmann *et al.*, Proc. 3rd Intern. Protactinium Conf. Schloss Elman, Germany (1969).
[60]N. Trautmann *et al.*, Z. Nat. a 23, 2127 (1968).
[61]C. M. Lederer *et al.*, Nucl. Phys. A 135, 36 (1969).
[62]S. A. Baranov *et al.*, Zh. Éksp. Teor. Fiz. 43, 1135 (1962) [Sov. Phys. JETP 16, 801 (1963)].
[63]A. Backlin *et al.*, Lund. Proc. Intern. Symp. Neutron Capture Gamma-Ray Spectr., Studsvik, IAEA (1969), p. 141.
[64]W. R. Kane *et al.*, Phys. Rev. Lett. 25, 953 (1970).
[65]J. S. Boyno *et al.*, Bull. Amer. Phys. Soc. 17, 463 (1972).
[66]K. Katori *et al.*, Phys. Rev. C 8, 2336 (1973).
[67]S. A. Baranov *et al.*, Yad. Fiz. 1, 557 (1965) [Sov. J. Nucl. Phys. 1, 397 (1965)].
[68]F. S. Stephens *et al.*, in: Coulomb Excitation (eds. K. Alder and W. Winter), Academic Press, New York (1966), p. 208.
[69]R. M. Diamond and F. S. Stephens, Arkiv. Fys. 36, 221 (1967).
[70]A. B. Smith, Nucl. Phys. 47, 633 (1963).
[71]E. Barnard *et al.*, Nucl. Phys. 80, 46 (1966).
[72]A. T. G. Ferguson, Izv. Akad. Nauk SSSR, Ser. Fiz. 31, 74 (1967).
[73]A. M. Fridman *et al.*, Phys. Rev. C 9, 760 (1974).
[74]J. Borggreen *et al.*, Nucl. Phys. 29, 515 (1962).
[75]R. A. Glass *et al.*, J. Inorg. Nuclear Chem. 13, 181 (1960).
[76]B. S. Dzhelepov *et al.*, Zh. Éksp. Teor. Fiz. 45, 1360 (1963) [Sov. Phys. JETP 18, 937 (1964)].
[77]S. A. Baranov *et al.*, Yad. Fiz. 4, 1108 (1966) [Sov. J. Nucl. Phys. 4, 798 (1967)].
[78]S. A. Baranov *et al.*, Yad. Fiz. 10, 1110 (1969) [Sov. J. Nucl. Phys. 10, 632 (1970)].
[79]M. R. Schmorak *et al.*, Phys. Rev. Lett. 24, 1507 (1970).
[80]L. P. Bilibin *et al.*, Izv. Akad. Nauk SSSR, Ser. Fiz. 30, 217 (1966).
[81]M. R. Schmorak *et al.*, Phys. Rev. Lett. 24, 1507 (1970).
[82]S. W. Yates *et al.*, Bull. Amer. Phys. Soc. 20, 97 (1975).
[83]R. A. Meyer *et al.*, Bull. Amer. Phys. Soc. 17, 464 (1972).
[84]P. R. Fields *et al.*, Nucl. Phys. A 208, 269 (1973).
[85]G. N. Flerov *et al.*, At. Énerg. 17, 310 (1964) [Sov. Atomic Energy].

Translated by Julian B. Barbour